NACA

RESEARCH MEMORANDUM

STATIC LONGITUDINAL STABILITY CHARACTERISTICS OF A COMPOSITE-PLAN-FORM WING MODEL INCLUDING SOME COMPARISONS WITH A 45° SWEPTBACK WING AT TRANSONIC SPEEDS

By Walter D. Wolhart

Langley Aeronautical Laboratory
Langley Field, Va.

CLASSIFIED DOCUMENT

NATIONAL ADVISORY COMMITTEE FOR AERONAUTICS

WASHINGTON

August 18, 1954

NACA RM L54F24

NATIONAL ADVISORY COMMITTEE FOR AERONAUTICS

RESEARCH MEMORANDUM

STATIC LONGITUDINAL STABILITY CHARACTERISTICS OF A COMPOSITE-PLAN-FORM WING MODEL INCLUDING SOME COMPARISONS WITH A 45° SWEPTBACK WING AT TRANSONIC SPEEDS

By Walter D. Wolhart

SUMMARY

An investigation was made to determine the low-subsonic-speed static longitudinal stability characteristics of a composite-plan-form wing tested as a wing-fuselage combination and as a complete model. Also included in the investigation was a comparison of the transonic-speed characteristics of the composite-plan-form wing alone and the 45° sweptback wing from which the composite wing was derived.

At low subsonic speeds both the wing-fuselage combination and the complete model showed an unstable break occurring in the pitching-moment curve at moderate angles of attack which could be decreased or delayed to higher angles of attack by controlling the flow over the outboard wing panels with the use of wing slats or fences or a combination of slats and fences. Raising the horizontal tail resulted in a decrease in stability at moderate and high angles of attack which was attributed to the tail passing through the wing wake. Adding either wing slats or fences improved the static longitudinal stability for all tail heights investigated and provided a stable pitching-moment curve throughout the angle-of-attack range for the tail in the lowest position investigated.

At transonic speeds the conventional 45° sweptback wing was longitudinally unstable at zero lift. The composite-plan-form wing, on the other hand, was stable or neutrally stable at zero lift and the high-subsonic-speed pitching-moment characteristics of the wing were generally similar to the low-subsonic-speed characteristics of the wing-fuselage combination. Increasing Mach number from high subsonic to low supersonic values increased the lift coefficient at which pitch-up occurred on the composite-plan-form wing.

INTRODUCTION

The development of high-speed airplanes has resulted in the use of thin airfoil sections and large amounts of sweepback to obtain the required aerodynamic characteristics. These design features have for obvious reasons presented structural problems which must be solved by the airplane designer. The composite-plan-form sweptback wing model tested in the investigation reported herein is part of a general research program of the National Advisory Committee for Aeronautics to determine the aerodynamic characteristics of airplane configurations which show promise of meeting structural as well as aerodynamic characteristics for high-speed flight.

The composite-plan-form wing is derived from a conventional 45° sweptback wing of aspect ratio 6, taper ratio of 0.6, and NACA 65A009 airfoil section and differs from the conventional wing in that the portion of the wing inboard of the 40-percent spanwise station and rearward of the 40-percent-chord line is rotated 90° rearward; a flat section is added within the triangular segment formed. The trailing edge of this portion of the wing is formed by the rearward 60 percent of the basic NACA 65A009 airfoil section. It should be noted that the absolute thickness of the modified wing remains the same while the thickness-to-chord ratio at the wing-fuselage juncture is reduced to approximately 4 percent. This wing has the structural advantages of a large root chord with the promise of maintaining the aerodynamic characteristics of a thin sweptback wing required for high-speed flight.

The investigation reported herein presents the low-subsonic- and transonic-speed static longitudinal stability characteristics of the composite-plan-form wing model. Transonic longitudinal stability characteristics of the conventional 45° sweptback wing are also presented. The low-subsonic-speed data were obtained from tests made in the Langley stability tunnel of a wing-fuselage combination to determine the effects of wing nacelles, slat span, fence spanwise location, a combination of slats and fences, and flap configuration and deflection on the static longitudinal stability characteristics. Low-subsonic-speed results also are presented for a complete model configuration with the composite wing installed to determine the effects of horizontal-tail height with various combinations of slats, fences, and flaps. The transonic-speed data were obtained from wing-alone tests made in the Langley high-speed 7- by 10-foot tunnel by using small semispan models.

SYMBOLS

The data presented herein are in the form of standard NACA coefficients of forces and moments which are referred to the stability system of axes with the origin at the projection on the plane of symmetry of the quarter-chord point of the wing mean aerodynamic chord. Positive directions of forces, moments, and angular displacements are shown in figure 1. The coefficients and symbols are defined as follows:

C_L lift coefficient, L/qS

C_D drag coefficient, D/qS

C_m pitching-moment coefficient, $M/qS\bar{c}$

C_B bending-moment coefficient at plane of symmetry, $\frac{B}{q\frac{S}{2}\frac{b}{2}}$

L lift (twice measured lift for semispan model), lb

D drag (twice measured drag for semispan model), lb

M pitching moment (twice measured pitching moment for semispan model), ft-lb

B bending moment at plane of symmetry, ft-lb

q dynamic pressure, lb/sq ft

V free-stream velocity, ft/sec

M free-stream Mach number

ρ mass density of air, slugs/cu ft

S total wing area (twice area for semispan model) sq ft

c chord measured parallel to plane of symmetry, ft

y spanwise distance measured perpendicular to plane of symmetry, ft

[redacted]

$\bar{c}$	wing mean aerodynamic chord, $\frac{2}{S}\int_0^{b/2} c^2 dy$, ft
b	wing span (twice span for semispan model), ft
y_{cp}	lateral center of pressure, measured at zero lift, percent of semispan
$\frac{\partial C_L}{\partial \alpha}$	lift-curve slope per degree, measured at zero lift
$\frac{\partial C_m}{\partial C_L}$	static-longitudinal-stability parameter, measured at zero lift
$C_{D_{C_L=0}}$	drag coefficient at zero lift
$(L/D)_{max}$	maximum lift-drag ratio
α	angle of attack, deg
δ	flap deflection, measured from wing-chord plane, deg

Abbreviations:

W	wing, used with subscripts 1 and 2 to denote the conventional 45° sweptback wing and the composite wing, respectively
F	fuselage
V	vertical tail
H	horizontal tail, used with subscripts H, L, or M to denote tail position (see fig. 2)
N	wing nacelles
Δ	triangular filler (see fig. 5)
s	slat, used with subscripts 1 to 3 to denote slat span (see fig. 4)

[redacted]

f fence, used with subscripts 1 to 3 to denote fence spanwise location (see fig. 4)

A, B flap configuration (see fig. 5)

APPARATUS AND TESTS

Low-speed tests.- The low-speed tests were made in the 6- by 6-foot test section of the Langley stability tunnel. The model was mounted on a single strut support with the pivot point located at the projection on the plane of symmetry of the quarter-chord point of the wing mean aerodynamic chord. Forces and moments were measured by a conventional six-component balance system.

The model tested was constructed primarily of mahogany with aluminum bulkheads and reinforcements. Geometric characteristics of this model are given in figures 2 to 5 and table I. The composite-plan-form wing was derived from a conventional 45° sweptback wing of aspect ratio 6, taper ratio of 0.6, and NACA 65A009 airfoil section parallel to the plane of symmetry and differs from the conventional wing in that the portion of the wing inboard of the 40-percent spanwise station and rearward of the 40-percent-chord line is rotated 90° rearward; a flat section is added within the triangular segement formed. The trailing edge of this portion of the wing is formed by the rearward 60 percent of the basic NACA 65A009 airfoil section. (See fig. 3.) The coordinates of the fuselage which was a body of revolution having a fineness ratio of 12.41 are presented in table I. The horizontal and vertical tails had flat-plate airfoil sections with rounded leading edges and beveled trailing edges. The wing nacelle location and coordinates are given in figure 2 and table I, respectively. Details of the slats and fence are given in figure 4. Most of the tests were made with a triangular filler added to the wing trailing edge at the 0.40b/2 station. This triangular filler is shown in figure 5 along with the plain split-flap configurations tested.

Tests were made of the wing-fuselage combination to determine the effects of wing nacelles, slats, flaps, and fences. The remaining tests were made on the complete model which included vertical and horizontal tails to determine the effects of slats, flaps, and fences for two different horizontal-tail heights. Tests were made of the complete model in the clean condition for three different tail heights.

The low-speed tests were made at a dynamic pressure of 39.7 pounds per square foot which corresponds to a Mach number of 0.16 and a Reynolds number of 1.98×10^6 based on the wing mean aerodynamic chord of 1.62 feet. The tests were made at 0° angle of sideslip for an angle-of-attack range from approximately -4° to 30°.

Approximate jet-boundary corrections have been applied to the angle of attack and to the drag coefficient by the method of reference 1. The pitching-moment correction for horizontal-tail-on configurations was obtained from reference 2. Blockage corrections have been applied to the data by using reference 3. No tare corrections for the effects of strut interference have been applied since these corrections were found to be negligible.

High-speed tests.- The high-speed tests were made in the Langley high-speed 7- by 10-foot tunnel with small semispan models. These models were wing-alone models of the composite-plan-form wing W_2 and the conventional 45° sweptback wing W_1 from which the composite-plan-form wing was derived (see figs. 3 and 6). The conventional 45° sweptback wing model was made of beryllium copper. The composite-plan-form wing was obtained by adding a brass-bismuth-tin-alloy section to the basic wing. The models were mounted on a reflection-plane plate (fig. 7) which was located 3 inches from the tunnel wall in order to bypass the tunnel-wall boundary layer. For Mach numbers below $M = 0.95$, the flow field was essentially free of velocity gradients. At the higher Mach numbers, however, the presence of the reflection-plane plate created a high-local-velocity field which allowed testing the small models up to a Mach number of 1.10 before choking occurred in the tunnel. Further details of the test technique and Mach number gradients may be found in reference 4. The Mach number range was 0.7 to 1.09, corresponding to a Reynolds number range of approximately 1.07×10^6 to 1.25×10^6 based on the mean aerodynamic chord of the composite-plan-form wing.

No attempt has been made to apply corrections for jet-boundary or blockage effects. Because of the small size of the models these corrections are believed to be negligible. Corrections due to aeroelastic effects were less than 1.0 percent and were not applied to the data.

RESULTS AND DISCUSSION

Presentation of Results and General Remarks

The low-speed results of the present investigation are presented as the variation of C_L, C_D, and C_m with α in figures 8 to 19. The high-speed results are presented as the variation of α, C_D, C_m, and and C_B with C_L in figure 20 and are summarized in figure 21. In general the discussion is confined to pitching-moment characteristics since this parameter is considered the most important for this investigation. As an aid to the reader in making a more detailed analysis, a summary of the configurations investigated and the figures giving data for these configurations is presented in table II.

[redacted]

Low-Speed Static Longitudinal Stability Characteristics

Wing-fuselage combination.- As shown in table II most of the tests were made with a small triangular filler (Δ) added to the composite-planform wing (fig. 5). In view of the small effect on the longitudinal stability characteristics of adding the triangular filler, the results with or without the filler added are considered to be the same. See figures 8 and 9.

The effects of adding wing nacelles at the 40-percent spanwise station are shown in figure 8. Adding the nacelles improved the lift characteristics slightly up to an angle of attack of about 24° and increased the lift-curve slope, measured through $\alpha = 0^\circ$, from 0.0510 to 0.0545. The unstable break in the pitching-moment curve, or pitch-up, was delayed from about $\alpha = 9^\circ$ to $\alpha = 11^\circ$ when the nacelles were added. The unstable break in the C_m curve is attributed to stalling of the outboard wing panels normally associated with sweptback wings at moderate and high angles of attack. A brief investigation with surface tufts indicated a spanwise flow toward the wing tips, resulting in premature tip stalling. The nacelles acted somewhat like a fence in alleviating this spanwise flow.

Most of the remaining tests for the wing-fuselage combination were aimed at eliminating the undesirable pitch-up characteristics by incorporating wing modifications such as slats or fences. Some effects of flap configuration and deflection are included for the sake of completeness.

The effects of variation in slat span ($s_1 = 0.34b/2$, $s_2 = 0.65b/2$, and $s_3 = 0.89b/2$) are shown in figure 9. These results show that the s_1 slats are the most effective in delaying the unstable break in the C_m curve and resulted in a stable or neutrally stable C_m curve up to an angle of attack of about 22°. Increasing the slat span resulted in corresponding decreases in the longitudinal stability although they showed some improvement over the basic wing-fuselage characteristics.

The effects of locating fences at various spanwise stations ($f_1 = 0.54b/2$, $f_2 = 0.61b/2$, and $f_3 = 0.68b/2$) are shown in figure 10. Controlling the spanwise flow over the outboard wing panels by adding wing fences delayed the unstable break in the pitching moment from about $\alpha = 9^\circ$ to $\alpha = 20^\circ$ for all fence spanwise locations investigated. Although fences f_3 are the most effective at angles of attack above about 20°, fences f_1 or f_2 provided slightly more stability at moderate angles of attack. The f_2 fences are considered to be a good compromise and are the ones used for the comparison of slats and fences and a combination of slats and fences.

[redacted]

A comparison of s_1 slats and f_2 fences with a combination of these slats and fences (s_1f_2) is shown in figure 11. This comparison shows the fences alone provide the best pitching-moment characteristics for angles of attack up to about 16° but that slats alone are better at higher angles of attack. The combination of slats and fences provides a good compromise between slats-alone and fences-alone results throughout the angle-of-attack range.

Some effects of differences in flap configuration and deflection (see fig. 5) are shown in figure 12. A comparison of flap configurations A and B for $\delta = 60°$ indicates that flaps B were about twice as effective as flaps A in producing lift at $\alpha = 0°$ even though the geometric areas of the two flap configurations are comparable. However, flaps A maintained their lift effectiveness to higher angles of attack. The difference in effectiveness between flaps A and B at $\alpha = 0°$ is about what might be expected if it is remembered that the lift on a skewed flap is proportional to the cosine squared of the angle of sweepback of the hinge line. The lift effectiveness for flaps B is about 14 percent greater for $\delta = 40°$ than $\delta = 60°$ at $\alpha = 0°$. The effects of flap configuration and deflection on the pitching-moment characteristics are small and the curves are similar to those for the wing in the clean condition. The unstable break in the C_m curve occurs at about $\alpha = 7°$ for flaps deflected as compared to $\alpha = 9°$ for flaps undeflected.

A comparison of slats s_1 and fences f_2 with a combination of these slats and fences s_1f_2 is shown in figures 13 and 14 for flaps B deflected 60° and 40°, respectively. These wing modifications resulted in improved pitching-moment characteristics similar to those noted for the flaps-undeflected case.

Complete model.- The effects of horizontal-tail height for the model in the clean condition are shown in figure 15. All tail heights investigated show a destabilizing break in the C_m curve at about $\alpha = 11°$ which is attributed to stalling of the outboard wing panels as mentioned previously for the wing-fuselage combination. Raising the horizontal tail results in a decrease in stability at moderate and high angles of attack due to the horizontal tail passing through the wing wake. This effect of wing wake is also evident in the lift curves and results in decreased lift at moderate and high angles of attack for the higher tail positions. The effect on the pitching-moment characteristics of raising the horizontal tail is about what would be expected based on previous investigations of the effect of horizontal-tail height on sweptback wing models (for example, ref. 5).

The effects of adding slats s_1 and fences f_2 for the horizontal tail in the low and high positions are shown in figures 16 and 17, respectively. Adding either slats or fences improves the pitching-moment

characteristics for either tail height and provides a stable C_m curve throughout the angle-of-attack range for the tail in the low position. As before, raising the tail results in a decrease in stability at moderate and high angles of attack caused by the tail passing through the wing wake. The improved stability for either tail height when slats or fences are used is attributed to improved stability of the wing-fuselage combination and shows the fences are more effective at moderate angles of attack and the slats are more effective at high angles of attack. It is expected that a combination of slats and fences would provide a compromise throughout the angle-of-attack range as for the tail-off configuration.

The effects of adding slats s_1 and fences f_2 with flaps B deflected 40° and the horizontal tail in the low or high position are shown in figure 18 and 19, respectively. These results show that adding either slats or fences provides a stable C_m curve throughout the angle-of-attack range for the tail in the low position and in general has the same effects as noted for the flaps-undeflected case.

High-Speed Static Longitudinal Stability Characteristics of the Wing Alone

A comparison of the high-speed aerodynamic characteristics of the conventional sweptback wing and the composite-plan-form wing (wings W_1 and W_2, respectively) is shown in figure 20 and summarized in figure 21. In comparing these two wings it should be kept in mind that modifying the conventional 45° sweptback wing to give the composite-plan-form wing results in a decrease in aspect ratio from 6 to 4.06; therefore, the effects noted may be the result of aspect-ratio changes as well as plan-form changes. It should be noted that the high-subsonic-speed pitching-moment characteristics of the composite-plan-form wing alone are generally similar to the low-subsonic-speed characteristics of the wing-fuselage combination (figs. 8 and 20) and that increasing the Mach number from 0.70 to 1.09 increased the lift coefficient at which pitch-up occurs for this wing.

The zero-lift drag coefficient of the conventional wing is slightly less than that of the composite-plan-form wing for high subsonic Mach numbers as shown in figure 21. At low supersonic Mach numbers the composite-plan-form wing has a slightly lower $C_{D_{C_{L=0}}}$ which is attributed to the lower effective thickness of the root section. The conventional sweptback wing has higher $(L/D)_{max}$ ratios at the high subsonic speeds, but both wings have approximately the same value at low supersonic speeds.

[redacted]

The composite-plan-form wing has a higher lift-curve slope for Mach numbers greater than about 0.725 and shows a larger increase with increasing Mach number than the conventional wing which is partly attributed to the more rigid nature of the composite-plan-form wing. The plot $\frac{\partial C_m}{\partial C_L}$, measured through $C_L = 0$, against M shows that the composite-plan-form wing is stable or neutrally stable throughout the Mach number range. The conventional sweptback wing is unstable throughout the Mach number range and becomes very unstable for M above about 0.95. The lateral center of pressure y_{cp} is nearly constant throughout the Mach number range for the composite-plan-form wing whereas the conventional wing shows a large inboard shift beyond $M = 0.95$.

CONCLUSIONS

The results of a low-subsonic-speed investigation of the static longitudinal stability characteristics of a composite-plan-form wing-fuselage combination tested with and without the empennage installed and the results of a transonic-speed investigation of the composite-plan-form wing alone and the conventional 45° sweptback wing from which it was derived indicate the following conclusions:

1. In the low-subsonic-speed investigation with the composite-plan-form wing -

(a) For the model with or without the empennage installed, the results show an unstable break occurring in the pitching-moment curve at moderate angles of attack which could be decreased or delayed to higher angles of attack by controlling the flow over the outboard wing panels by the use of slats or fences or a combination of slats and fences. Deflecting plain split flaps had little effect on the pitching-moment characteristics.

(b) Raising the horizontal tail from a low to a high position resulted in a decrease in stability at moderate and high angles of attack due to the tail passing through the wing wake.

(c) With the horizontal tail in the low position, adding either wing slats or fences provides a stable pitching-moment curve throughout the angle-of-attack range.

2. In the transonic-speed investigation -

(a) At zero lift the conventional 45° sweptback wing was longitudinally unstable for the Mach number range investigated, this

condition being aggravated at the high Mach numbers. The composite-plan-form wing was stable or neutrally stable at zero lift throughout the Mach number range.

(b) The high-subsonic-speed pitching-moment characteristics of the composite-plan-form wing alone were generally similar to the low-subsonic-speed characteristics of the wing-fuselage combination. Increasing the Mach number from high subsonic to low supersonic values increased the lift coefficient at which pitch-up occurred on the composite-plan-form wing.

Langley Aeronautical Laboratory,
National Advisory Committee for Aeronautics
Langley Field, Va., June 15, 1954.

REFERENCES

1. Silverstein, Abe, and White, James A.: Wind-Tunnel Interference With Particular Reference to Off-Center Positions of the Wing and to the Downwash at the Tail. NACA Rep. 547, 1936.

2. Gillis, Clarence L., Polhamus, Edward C., and Gray, Joseph L., Jr.: Charts for Determining Jet-Boundary Corrections for Complete Models in 7- by 10-Foot Closed Rectangular Wind Tunnels. NACA WR L-123, 1945. (Formerly NACA ARR L5G31.)

3. Herriot, John G.: Blockage Corrections for Three-Dimensional-Flow Closed-Throat Wind Tunnels, With Consideration of the Effect of Compressibility. NACA Rep. 995, 1950. (Supersedes NACA RM A7B28).

4. Spreemann, Kenneth P., and Alford, William J., Jr.: Small-Scale Transonic Investigation of the Effects of Twist and Camber on the Aerodynamic Characteristics of a 60° 42' Sweptback Wing of Aspect Ratio 1.94. NACA RM L51I21, 1952.

5. Lichtenstein, Jacob H.: Experimental Determination of the Effect of Horizontal-Tail Size, Tail Length, and Vertical Location on Low-Speed Static Longitudinal Stability and Damping in Pitch of a Model Having 45° Sweptback Wing and Tail Surfaces. NACA Rep. 1096, 1952. (Supersedes NACA TN's 2381 and 2382.)

[redacted]

TABLE I

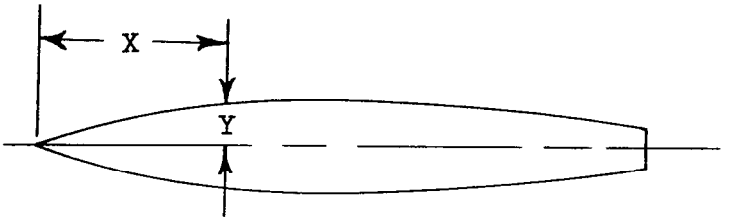

Fuselage Coordinates

X, in.	Y, in.
0	0
.4	.185
.6	.238
1.0	.342
2.0	.578
4.0	.964
6.0	1.290
8.0	1.577
12.0	2.074
16.0	2.472
20.0	2.772
24.0	2.993
28.0	3.146
32.0	3.250
36.0	3.314
40.0	3.334
44.0	3.304
48.0	3.219
52.0	3.307
56.0	2.849
60.0	2.661
64.0	2.474
68.0	2.302
72.0	2.141
76.0	1.982
80.0	1.819
83.0	1.695

Nacelle Coordinates

X, in.	Y, in.
0	0
.100	.070
.330	.169
.830	.336
1.300	.489
1.830	.622
2.330	.747
2.580	.800
2.958	.876
3.585	.974
4.840	1.105
6.095	1.190
7.350	1.240
8.605	1.255
16.830	1.255
17.872	1.237
18.913	1.195
19.955	1.127
20.996	1.029
22.038	.909
23.079	.768
24.121	.616
24.250	.598

[redacted]

TABLE II

STATIC LONGITUDINAL STABILITY CHARACTERISTICS

(a) Low-Speed Characteristics of Wing-Fuselage Combination

Configuration	Data presented	Figure
$W_2 + F$ $W_2 + F + N$	Effect of wing nacelles	8
$W_2 + F + \Delta$ $W_2 + F + \Delta + s_1$ $W_2 + F + \Delta + s_2$ $W_2 + F + s_3$	Effect of variation in slat span	9
$W_2 + F + \Delta$ $W_2 + F + \Delta + f_1$ $W_2 + F + \Delta + f_2$ $W_2 + F + \Delta + f_3$	Effect of variation in fence spanwise location	10
$W_2 + F + \Delta + f_2$ $W_2 + F + \Delta + s_1$ $W_2 + F + \Delta + s_1 + f_2$	Comparison of a fence and a slat configuration with a fence-slat combination	11
$W_2 + F + \Delta$ $W_2 + F + \Delta + A$, $\delta = 60^\circ$ $W_2 + F + \Delta + B$, $\delta = 60^\circ$ $W_2 + F + \Delta + B$, $\delta = 40^\circ$	Effect of flap configuration and deflection	12
$W_2 + F + \Delta + B$, $\delta = 60^\circ$, $+ f_2$ $W_2 + F + \Delta + B$, $\delta = 60^\circ$, $+ s_1$ $W_2 + F + \Delta + B$, $\delta = 60^\circ$, $+ s_1 + f_2$	Comparison of a fence and a slat configuration with a fence-slat combination for flaps B, $\delta = 60^\circ$	13
$W_2 + F + \Delta + B$, $\delta = 40^\circ$, $+ f_2$ $W_2 + F + \Delta + B$, $\delta = 40^\circ$, $+ s_1$ $W_2 + F + \Delta + B$, $\delta = 40^\circ$, $+ s_1 + f_2$	Comparison of a fence and a slat configuration with a fence-slat combination for flaps B, $\delta = 40^\circ$	14

[redacted]

TABLE II.- Concluded

STATIC LONGITUDINAL STABILITY CHARACTERISTICS

(b) Low-Speed Characteristics of Complete Model

Configuration	Data presented	Figure
$W_2 + F + V + H_L$ $W_2 + F + V + H_M$ $W_2 + F + V + H_H$	Effect of horizontal-tail height	15
$W_2 + F + \Delta + V + H_L + s_1$ $W_2 + F + \Delta + V + H_H + s_1$	Effect of horizontal-tail height with slat s_1	16
$W_2 + F + \Delta + V + H_L + f_2$ $W_2 + F + \Delta + V + H_H + f_2$	Effect of horizontal-tail height with fence f_2	17
$W_2 + F + \Delta + V + H_L + B, \delta = 40^\circ, + s_1$ $W_2 + F + \Delta + V + H_H + B, \delta = 40^\circ, + s_1$	Effect of horizontal-tail height with flap B, $\delta = 40^\circ$, and slat s_1	18
$W_2 + F + \Delta + V + H_L + B, \delta = 40^\circ, + f_2$ $W_2 + F + \Delta + V + H_H + B, \delta = 40^\circ, + f_2$	Effect of horizontal-tail height with flap B, $\delta = 40^\circ$, and fence f_2	19

(c) High-Speed Characteristics of Wing Alone

Configuration	Data presented	Figure
W_1 W_2	Comparison of conventional sweptback wing with composite-plan-form wing	20
W_1 W_2	Summary of results obtained with conventional sweptback wing and composite-plan-form wing	21

[redacted]

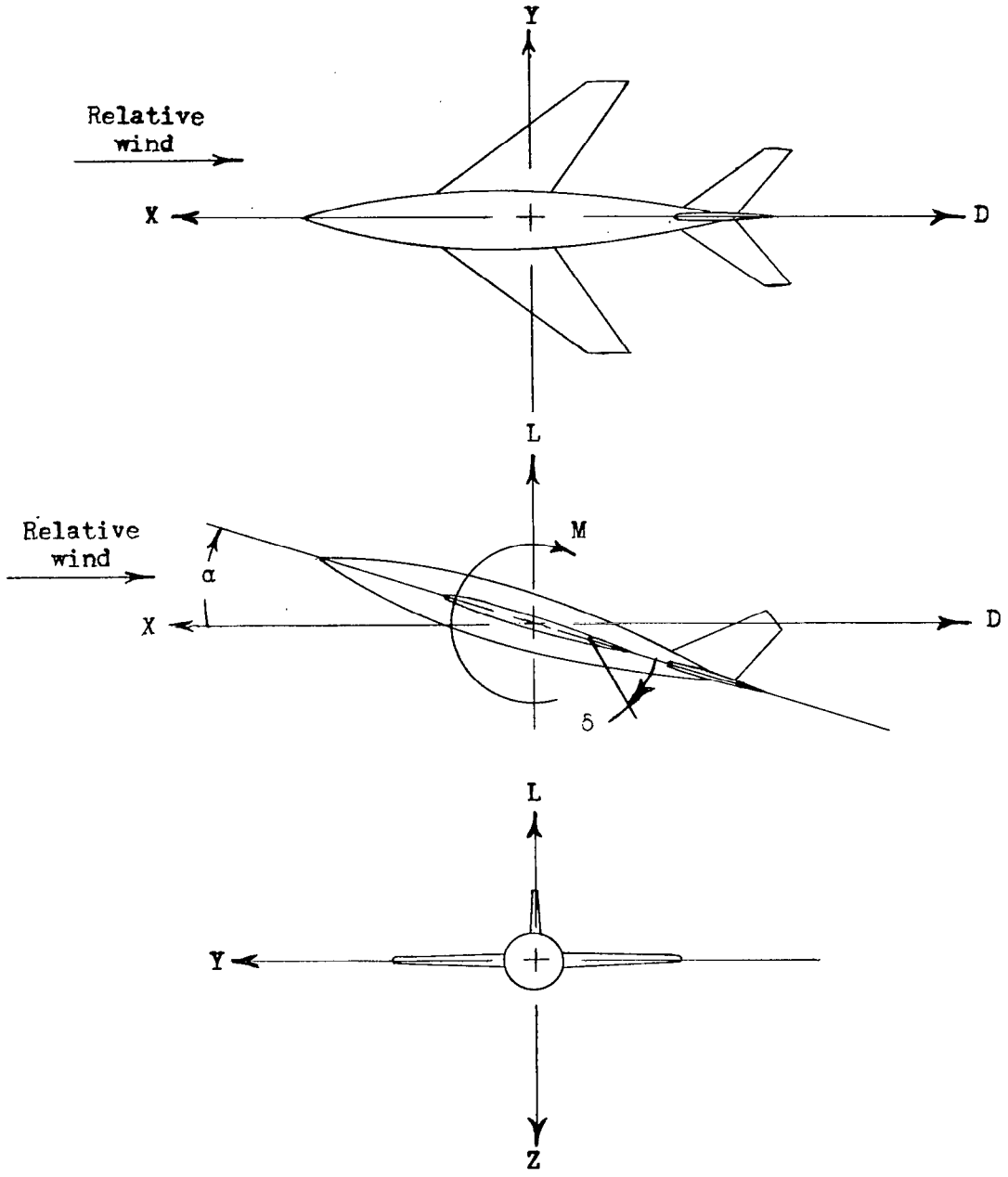

Figure 1.- System of axes used. Arrows indicate positive directions of forces, moments, and angular displacements.

[redacted]

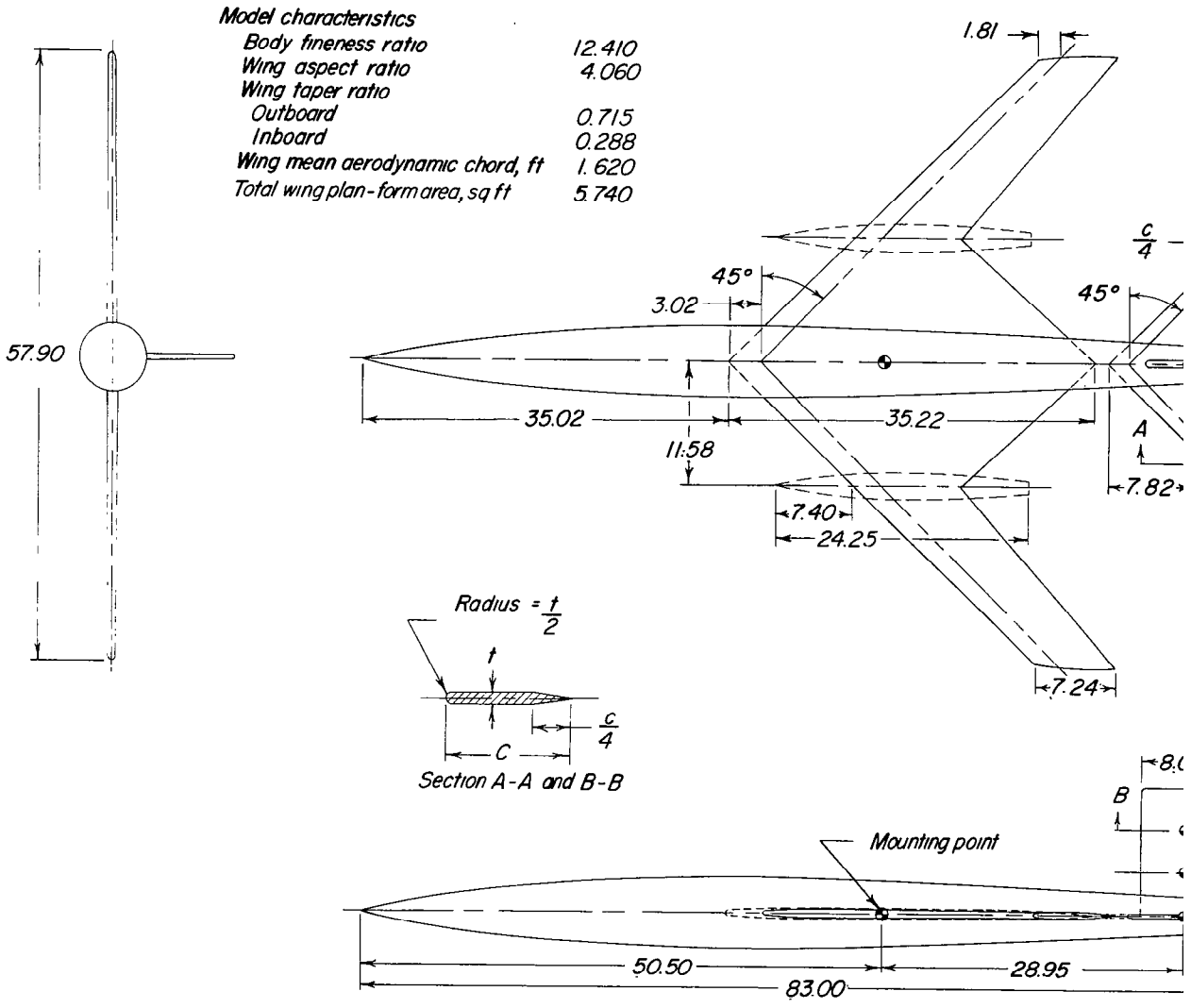

Figure 2.- Geometric characteristics of low-speed model. (All dime
are in inches unless otherwise specified.)

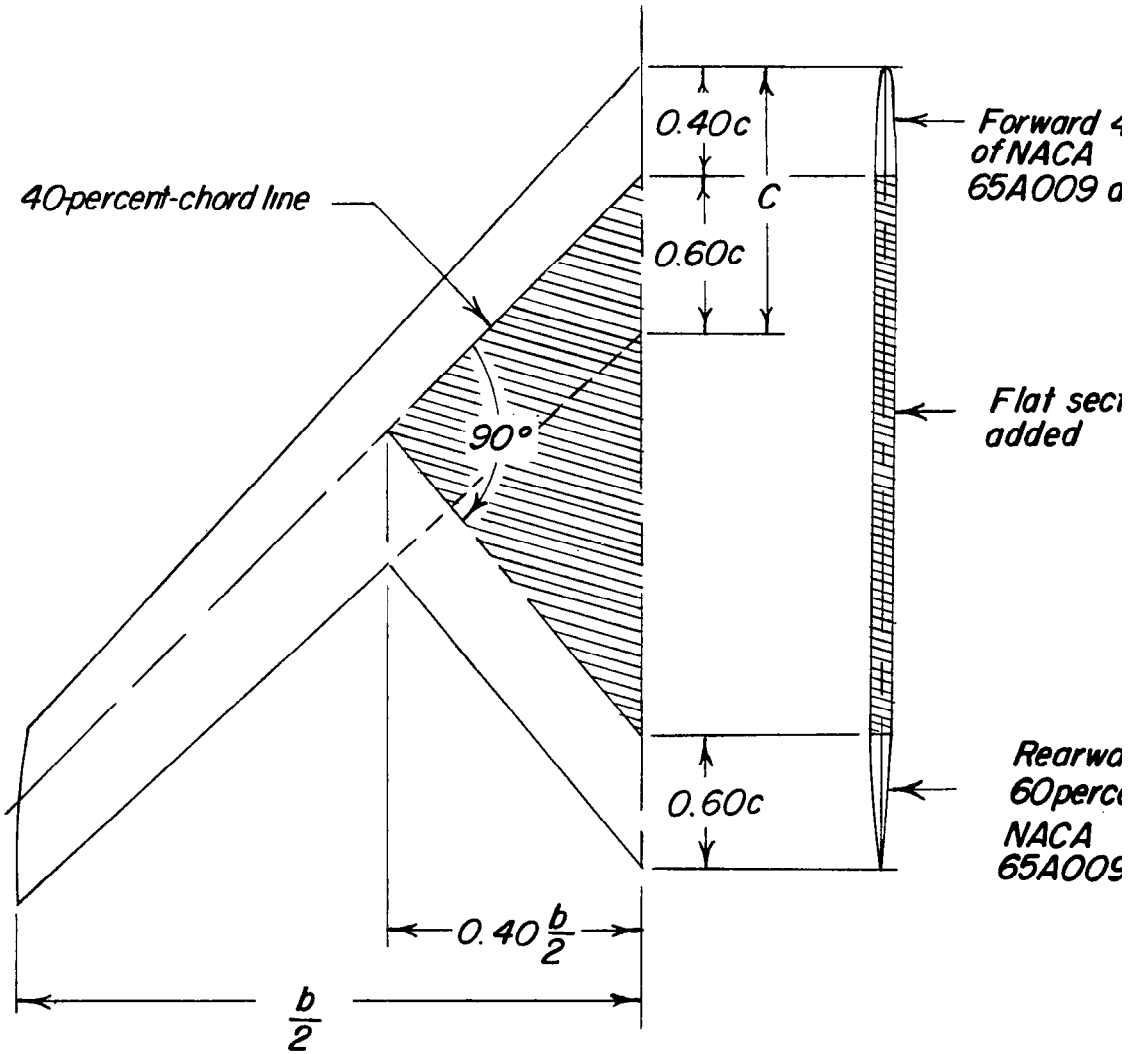

Figure 3.- Composite-plan-form wing of aspect ratio 4.06 derived 45° sweptback wing of aspect ratio 6 and taper ratio of 0.6.

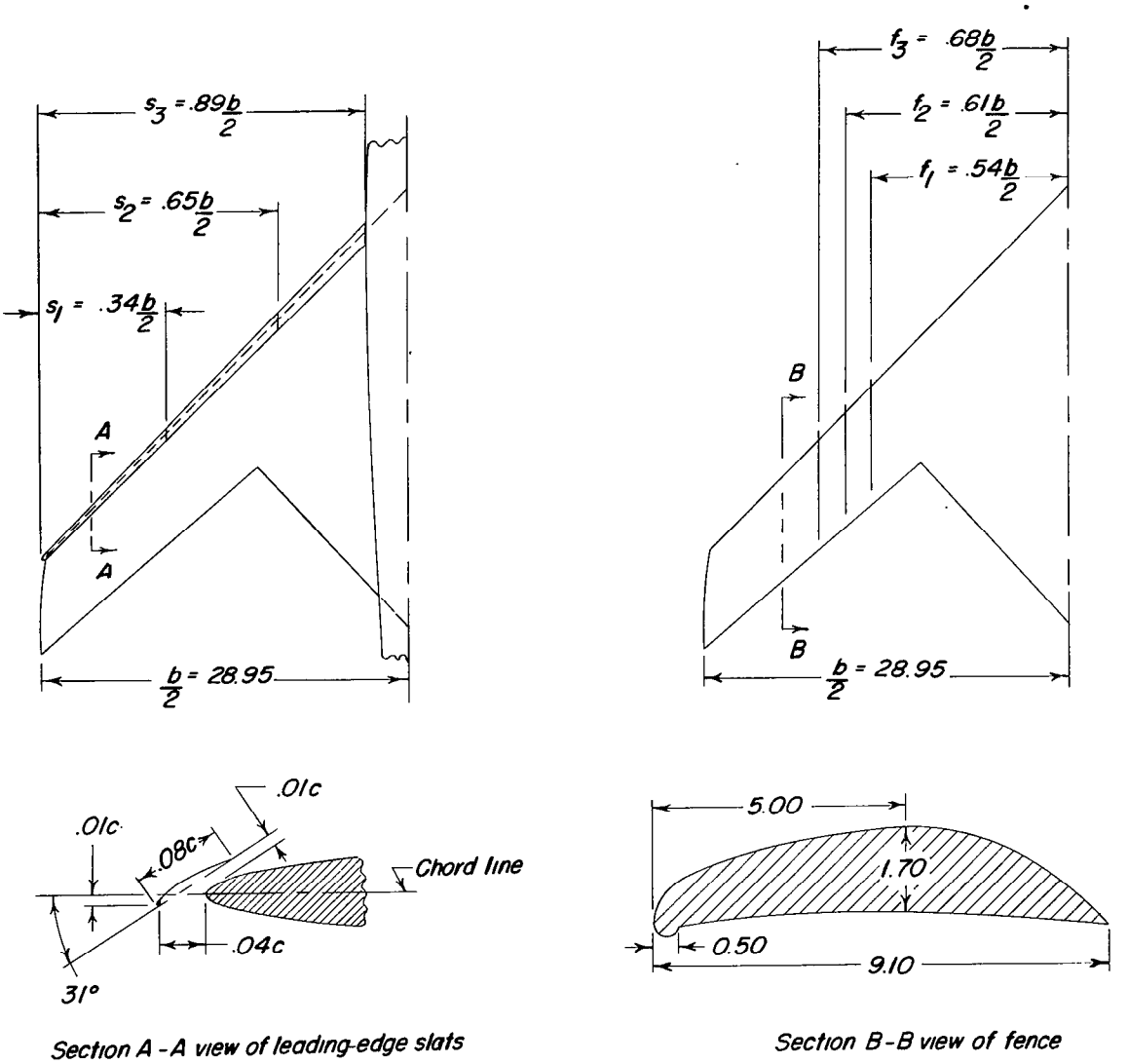

Section A-A view of leading-edge slats

Section B-B view of fence

Figure 4.- Details of wing slat and fence configurations for low-speed model.

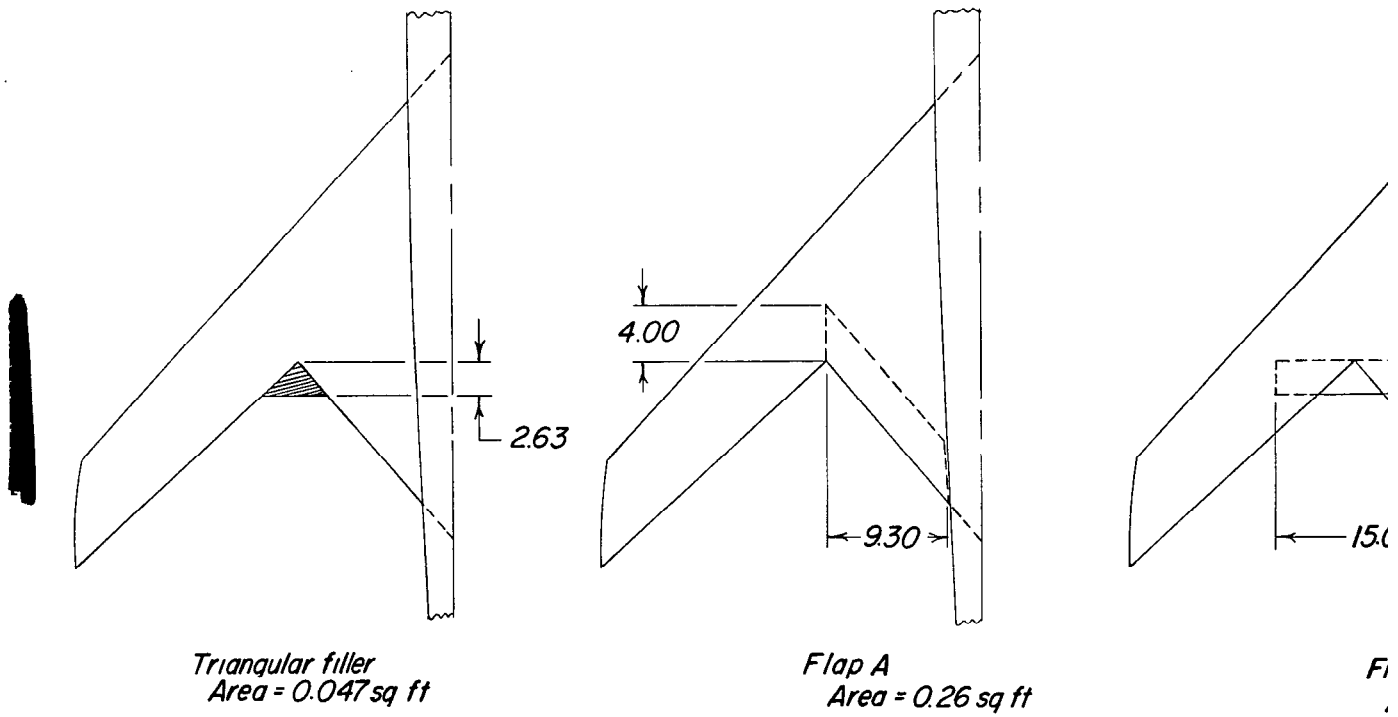

Figure 5.- Details of wing-plan-form modifications and flap configuratic
for low-speed model.

Characteristics of wing W_1

Aspect ratio	6.00
Taper ratio	0.60
Mean aerodynamic chord, ft	0.147
Area (twice semispan area), sq ft	0.125

Characteristics of win

Aspect ratio	
Taper ratio	
Outboard	
Inboard	
Mean aerodynamic cha	
Area(twice semispan ar	

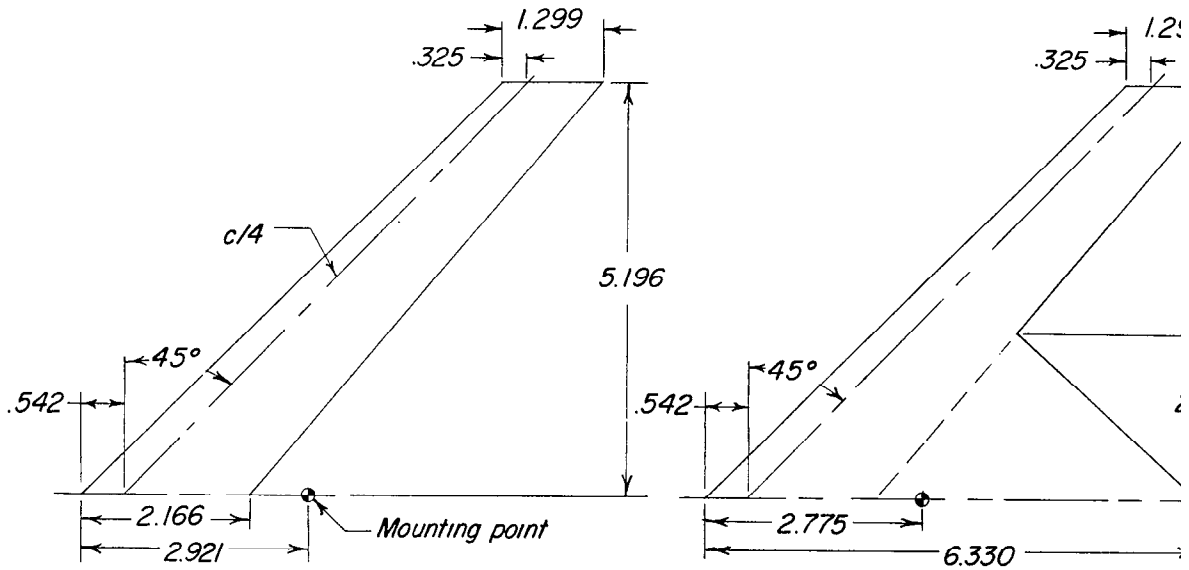

(a) Conventional sweptback wing, W_1.

(b) Composite-plan-form wing, W_2.

Figure 6.- Geometric characteristics of small-scale semispan models u in high-speed tests. (All dimensions are in inches unless otherwi specified.)

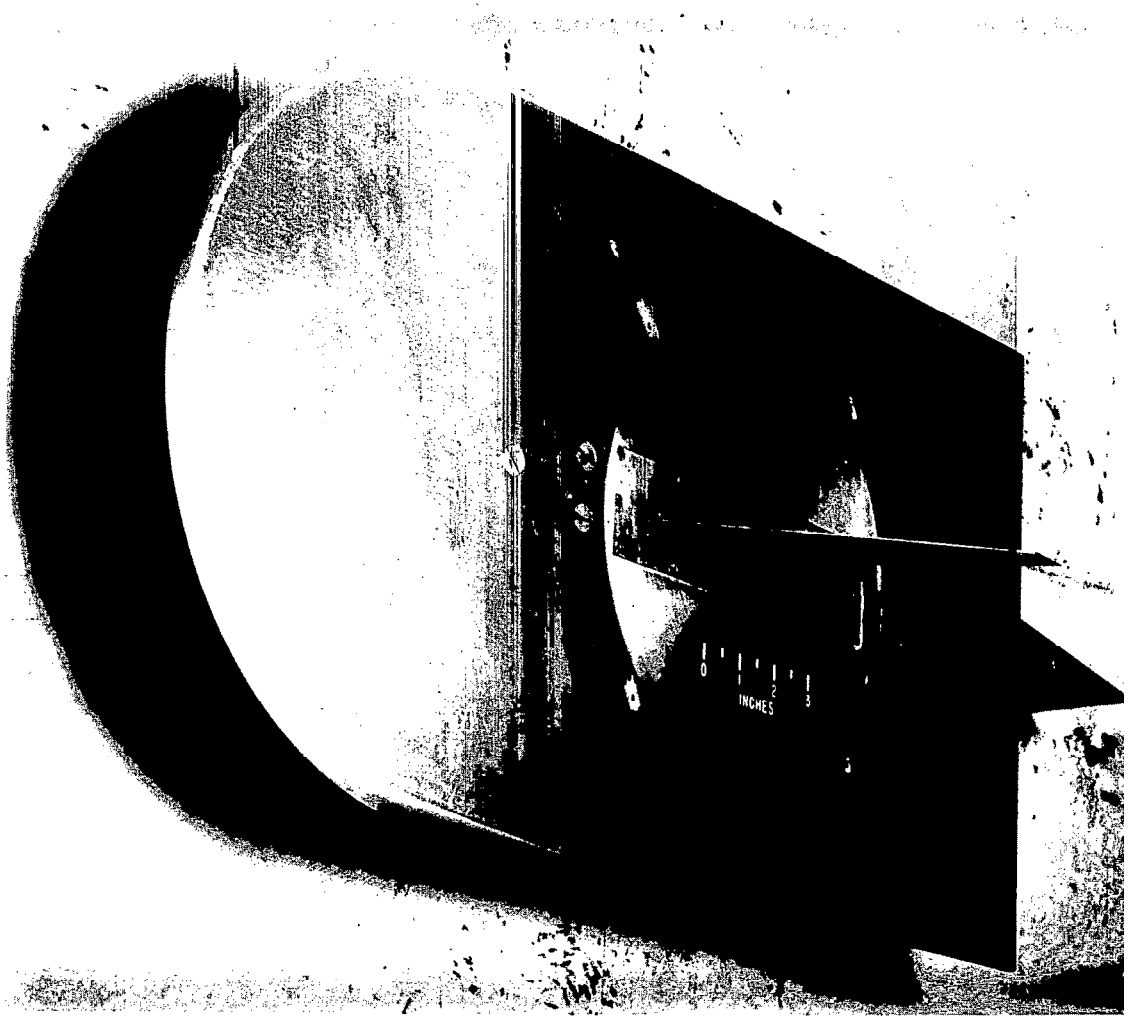

L-6736

Figure 7.- View of test model mounted on the reflection plane in t
Langley high-speed 7- by 10-foot tunnel.

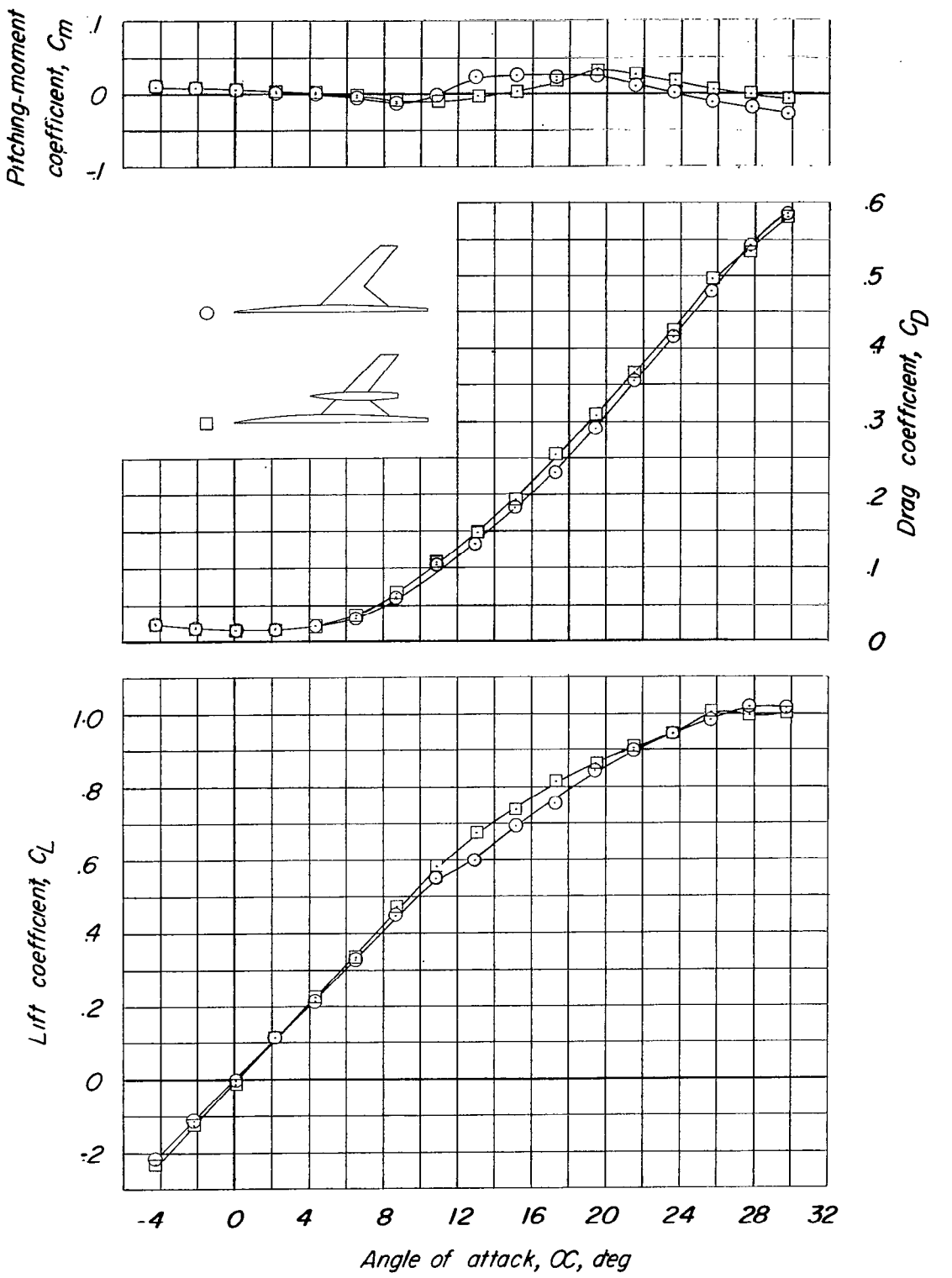

Figure 8.- Effect of wing nacelles on the static longitudinal stability characteristics of the wing-fuselage combination. M = 0.16.

[redacted]

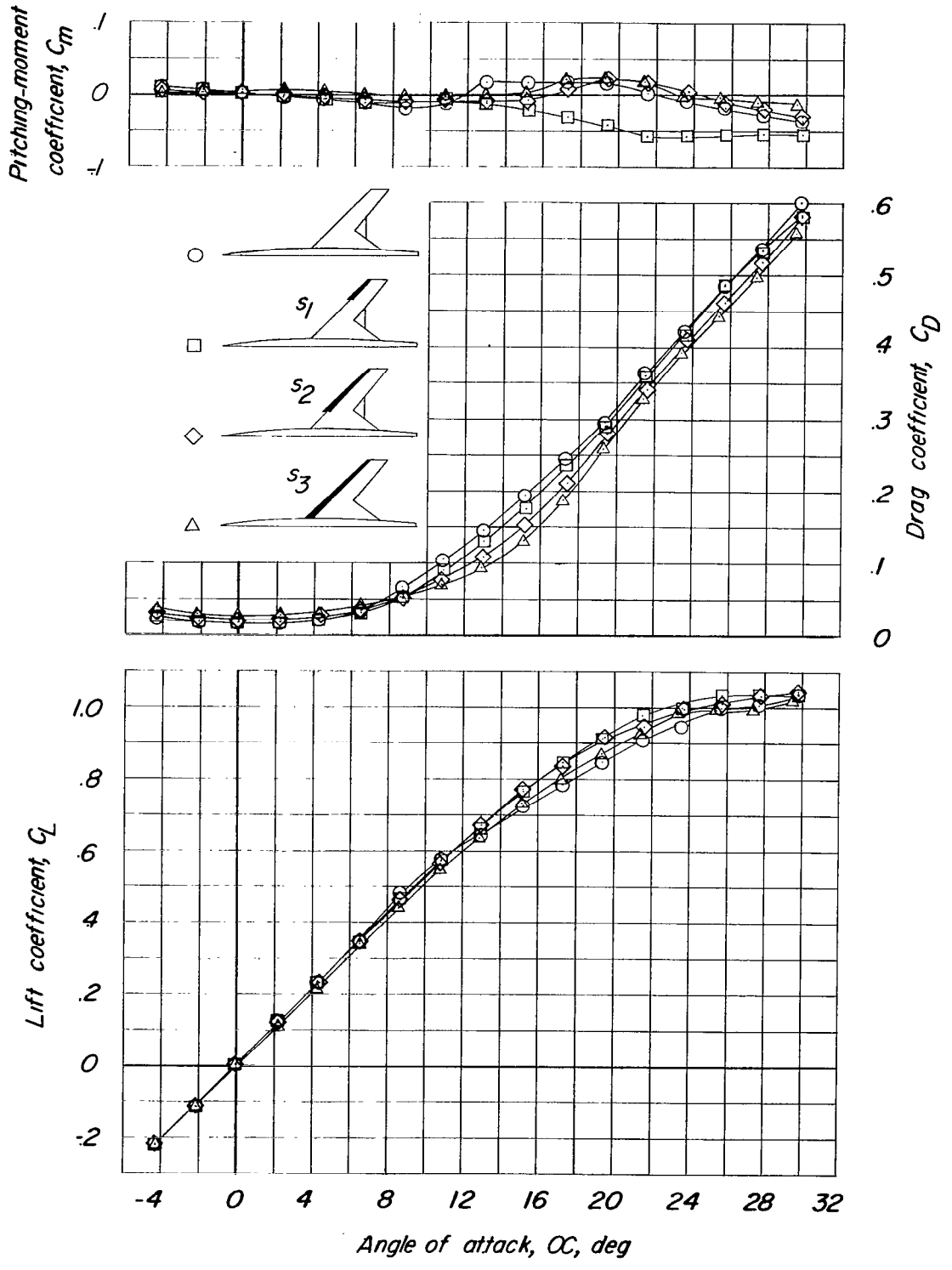

Figure 9.- Effect of variation in slat span on the static longitudinal stability characteristics of the wing-fuselage combination. M = 0.16.

[redacted]

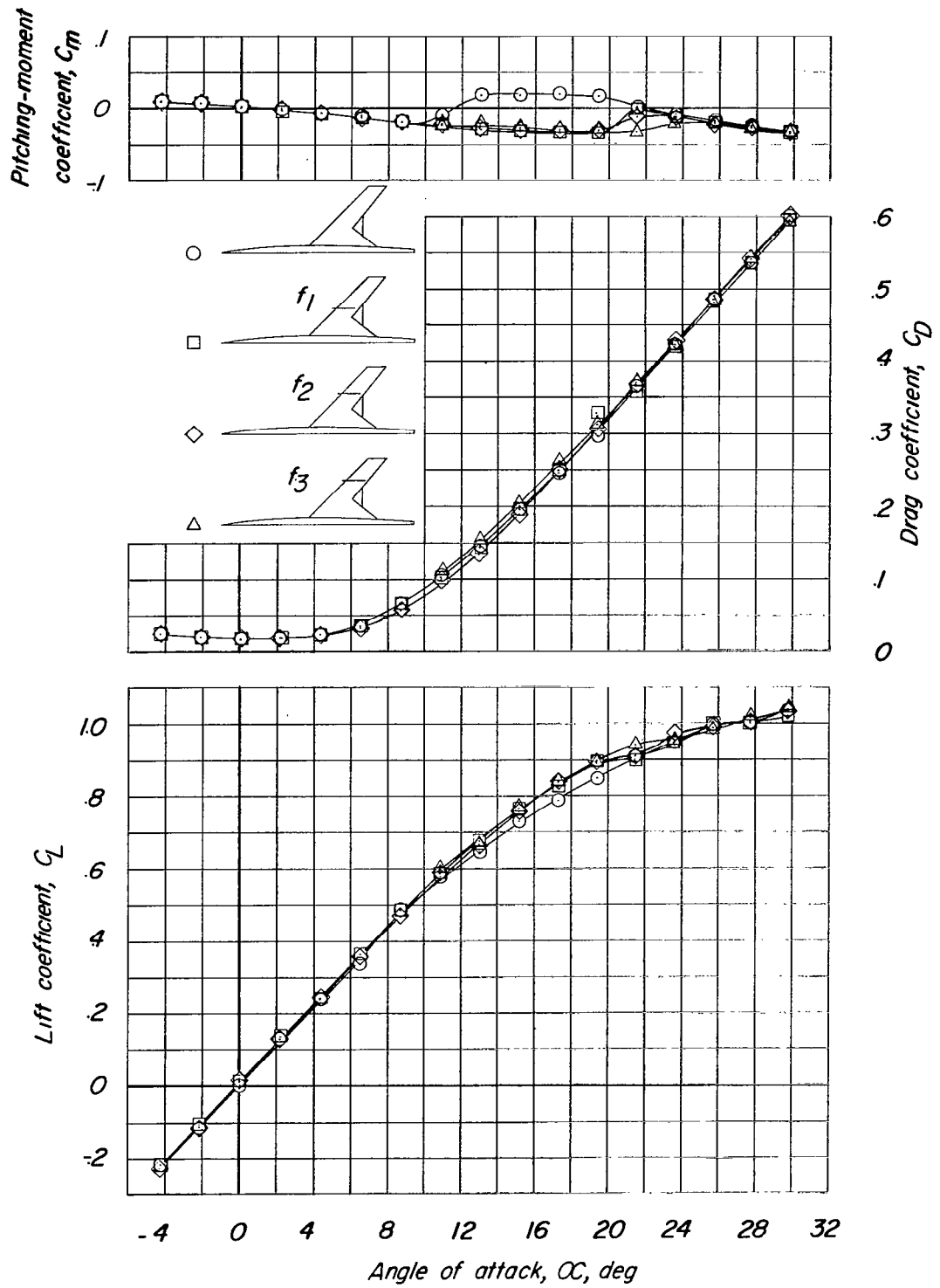

Figure 10.- Effect of variation in fence spanwise location on the static longitudinal stability characteristics of the wing-fuselage combination. M = 0.16.

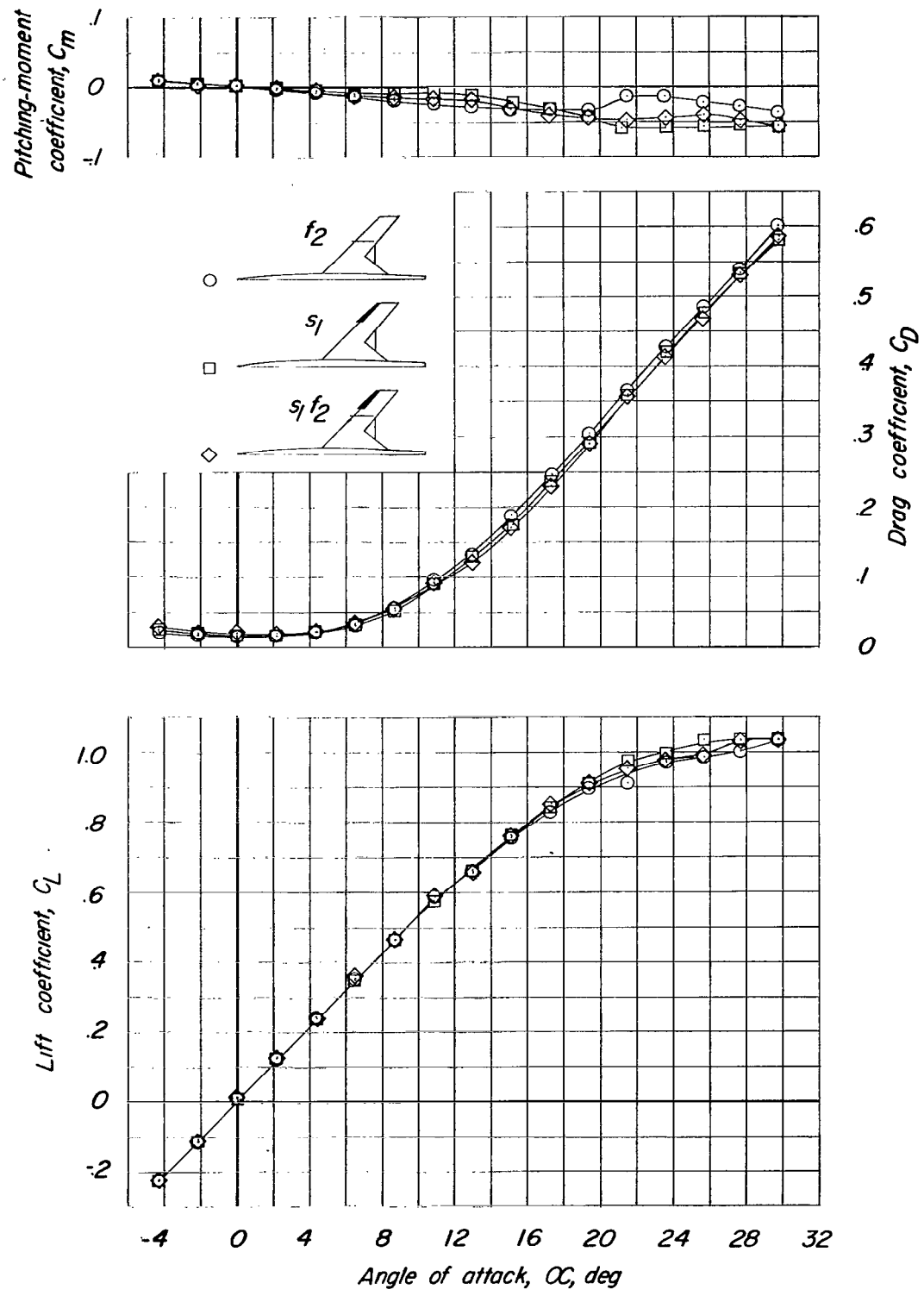

Figure 11.- Comparison of fences f_2 and slats s_1 with a combination of slats and fences $s_1 f_2$ for the wing-fuselage combination. M = 0.16.

[redacted]

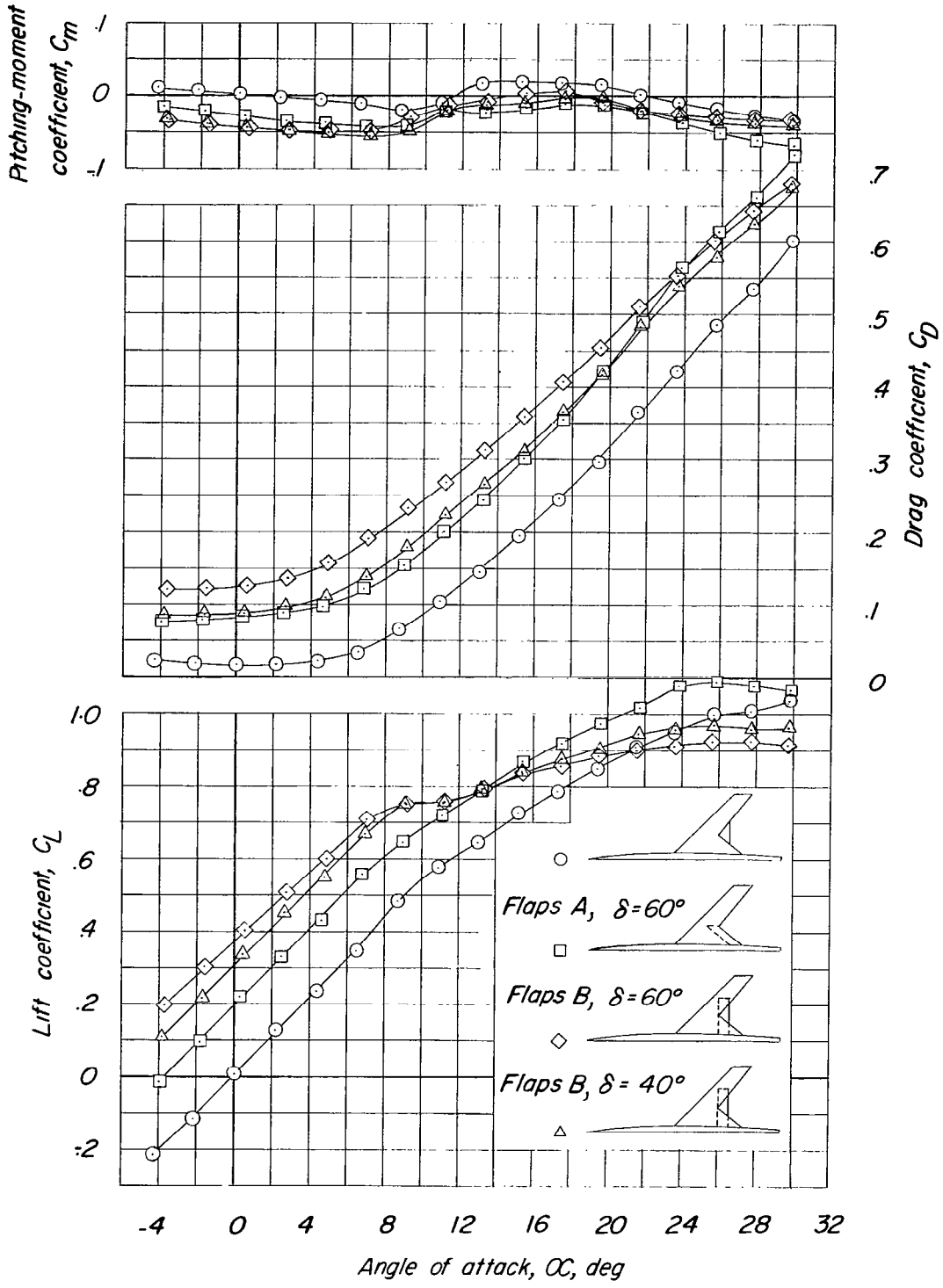

Figure 12.- Effect of flap deflection and configuration on the static longitudinal stability characteristics of the wing-fuselage combination. M = 0.16.

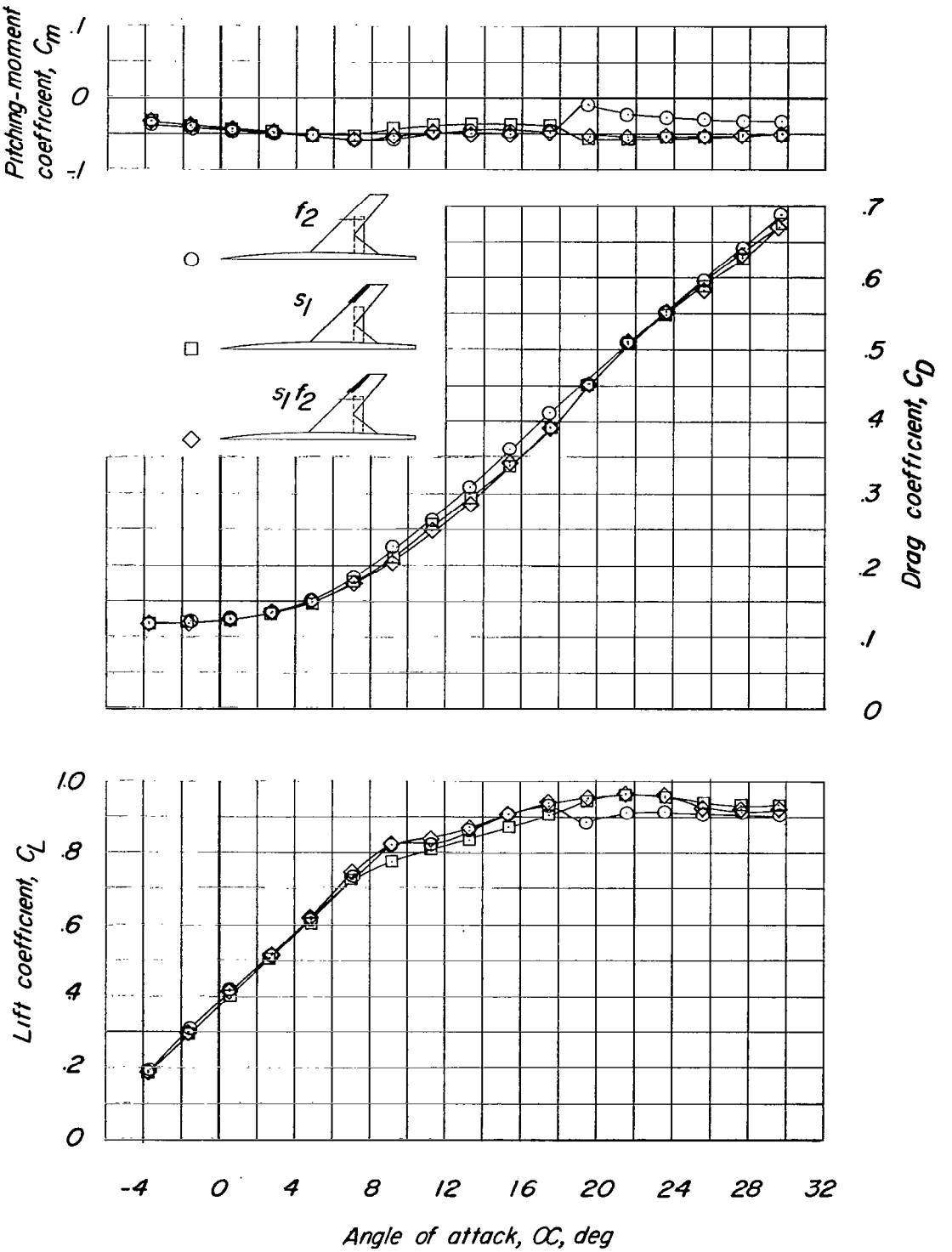

Figure 13.- Comparison of fences f_2 and slats s_1 with a combination of slats and fences $s_1 f_2$ for the wing-fuselage combination with flaps B, $\delta = 60^\circ$. M = 0.16.

[redacted]

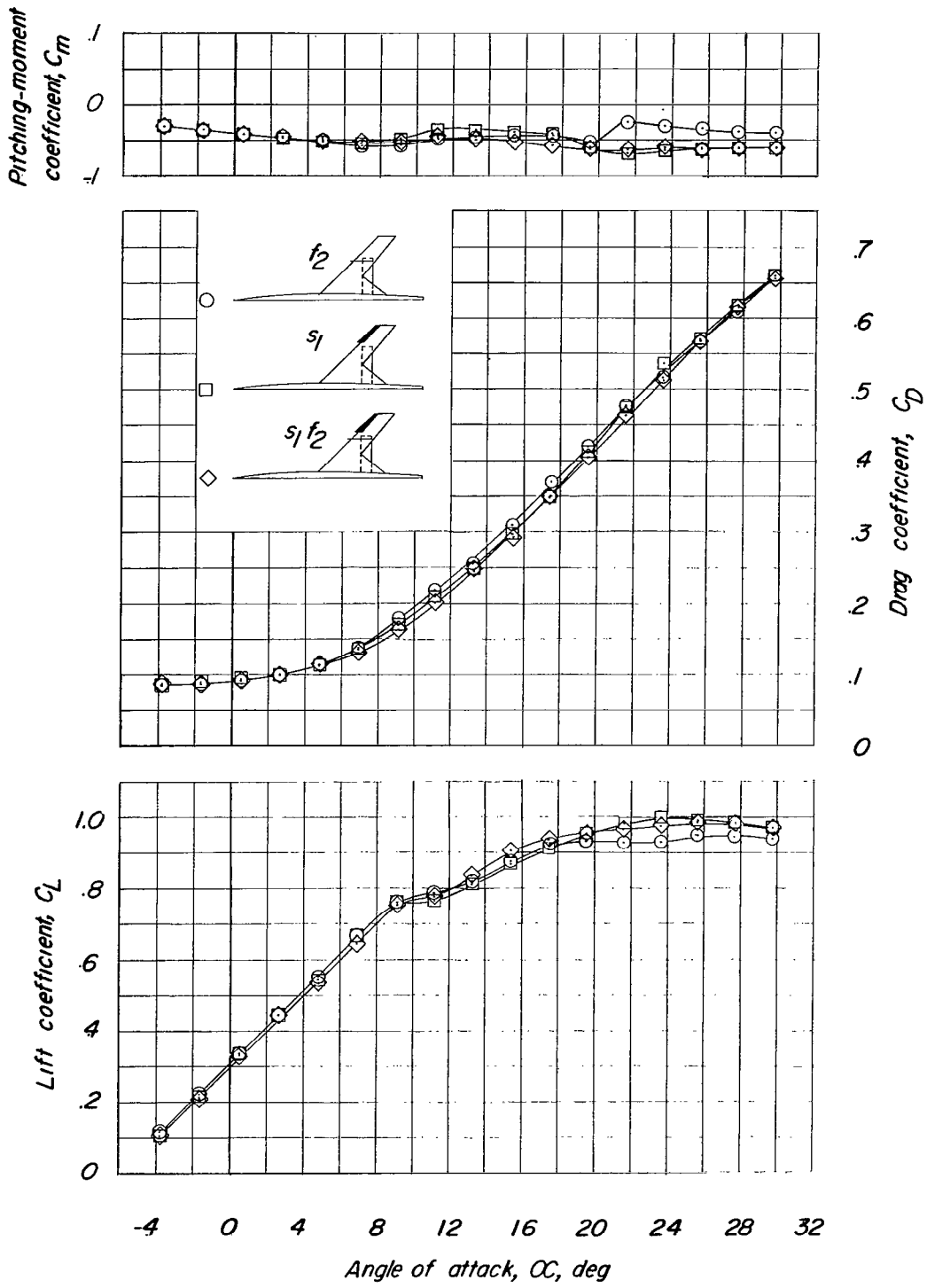

Figure 14.- Comparison of fences f_2 and slats s_1 with a combination of slats and fences $s_1 f_2$ for the wing-fuselage combination with flaps B, $\delta = 40^\circ$. M = 0.16.

[redacted]

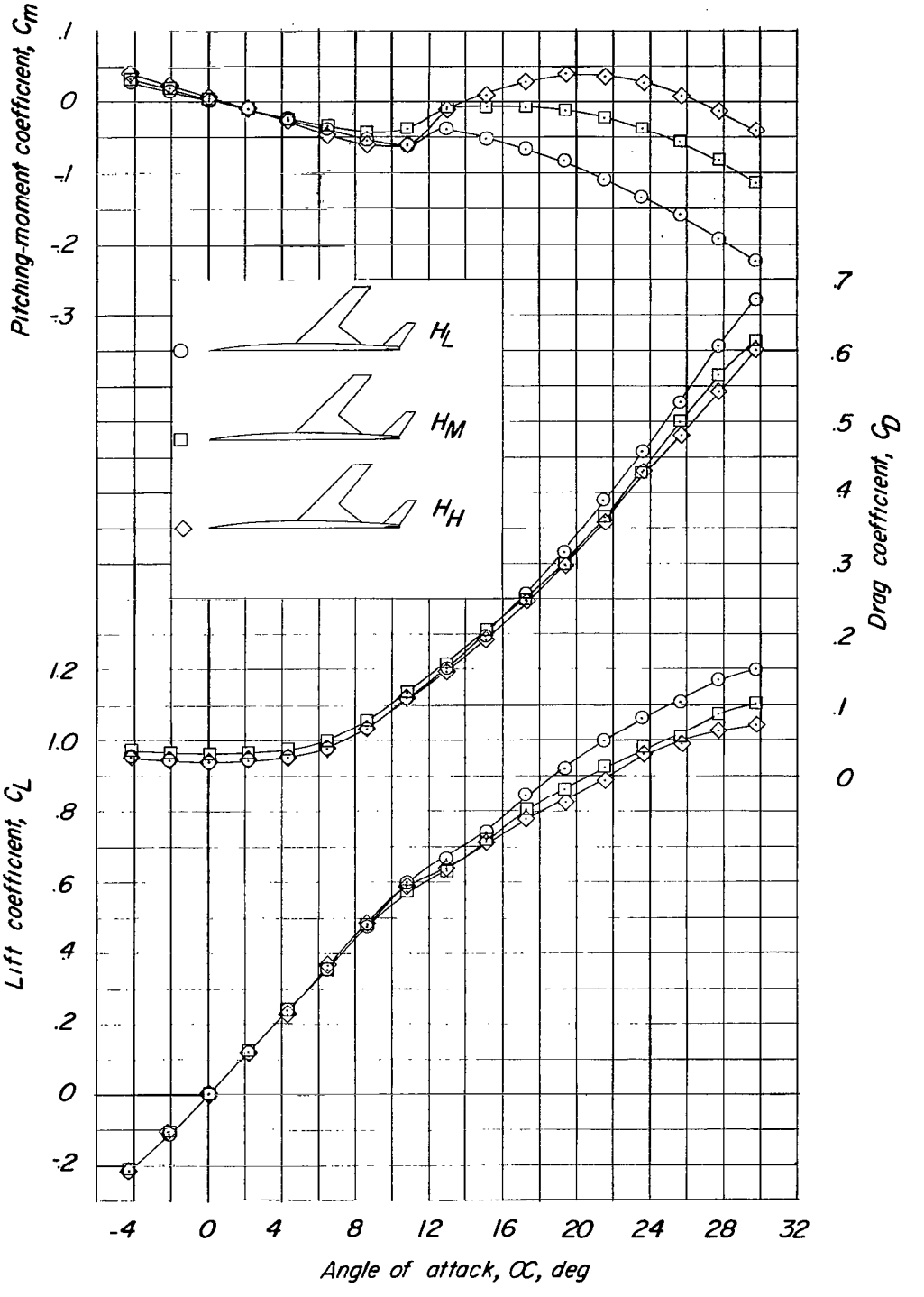

Figure 15.- Effect of horizontal-tail height on the static longitudinal stability characteristics of the complete model. M = 0.16.

[redacted]

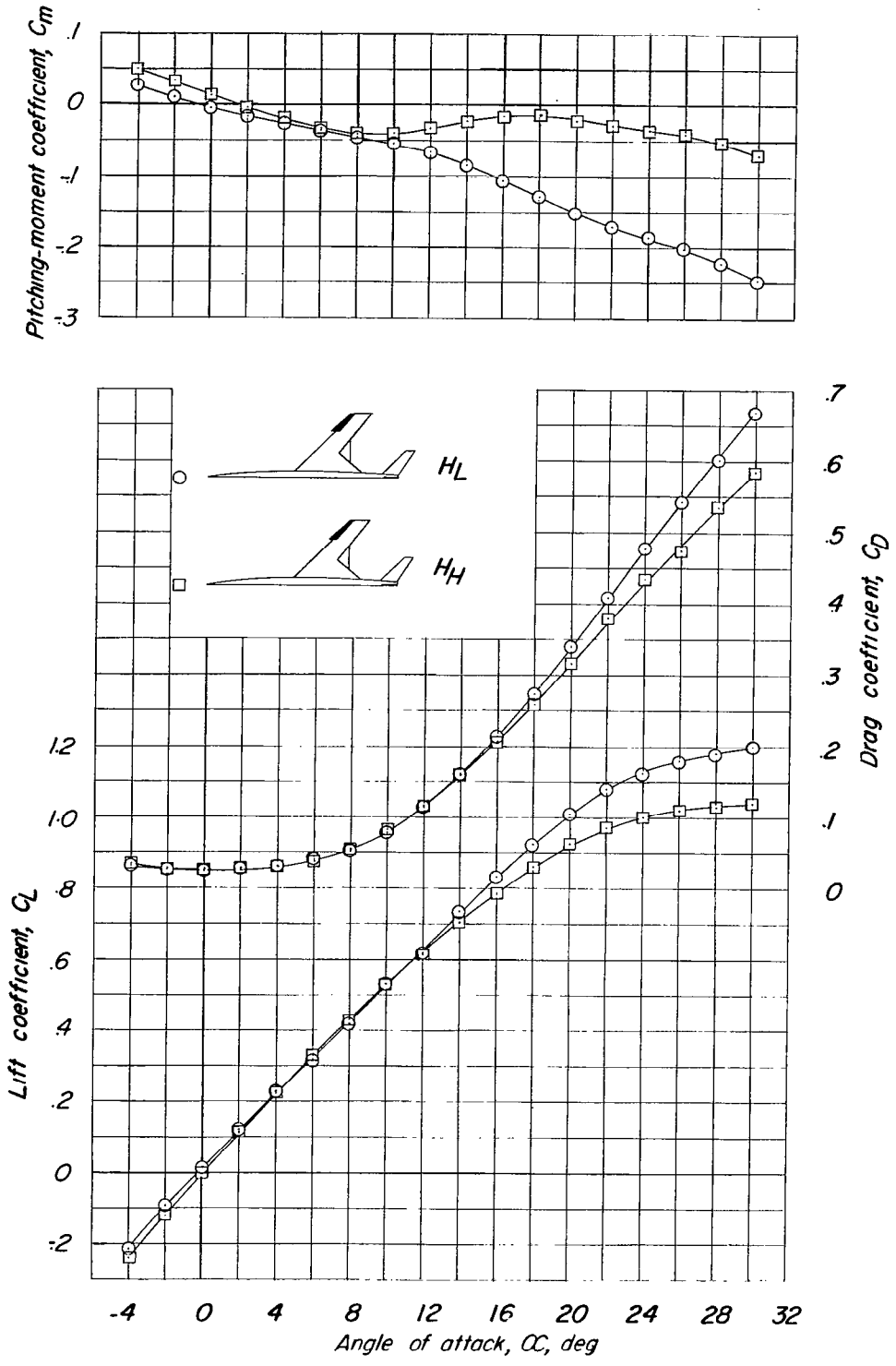

Figure 16.- Effect of horizontal-tail height on the static longitudinal stability characteristics of the complete model with slats s_1. M = 0.16.

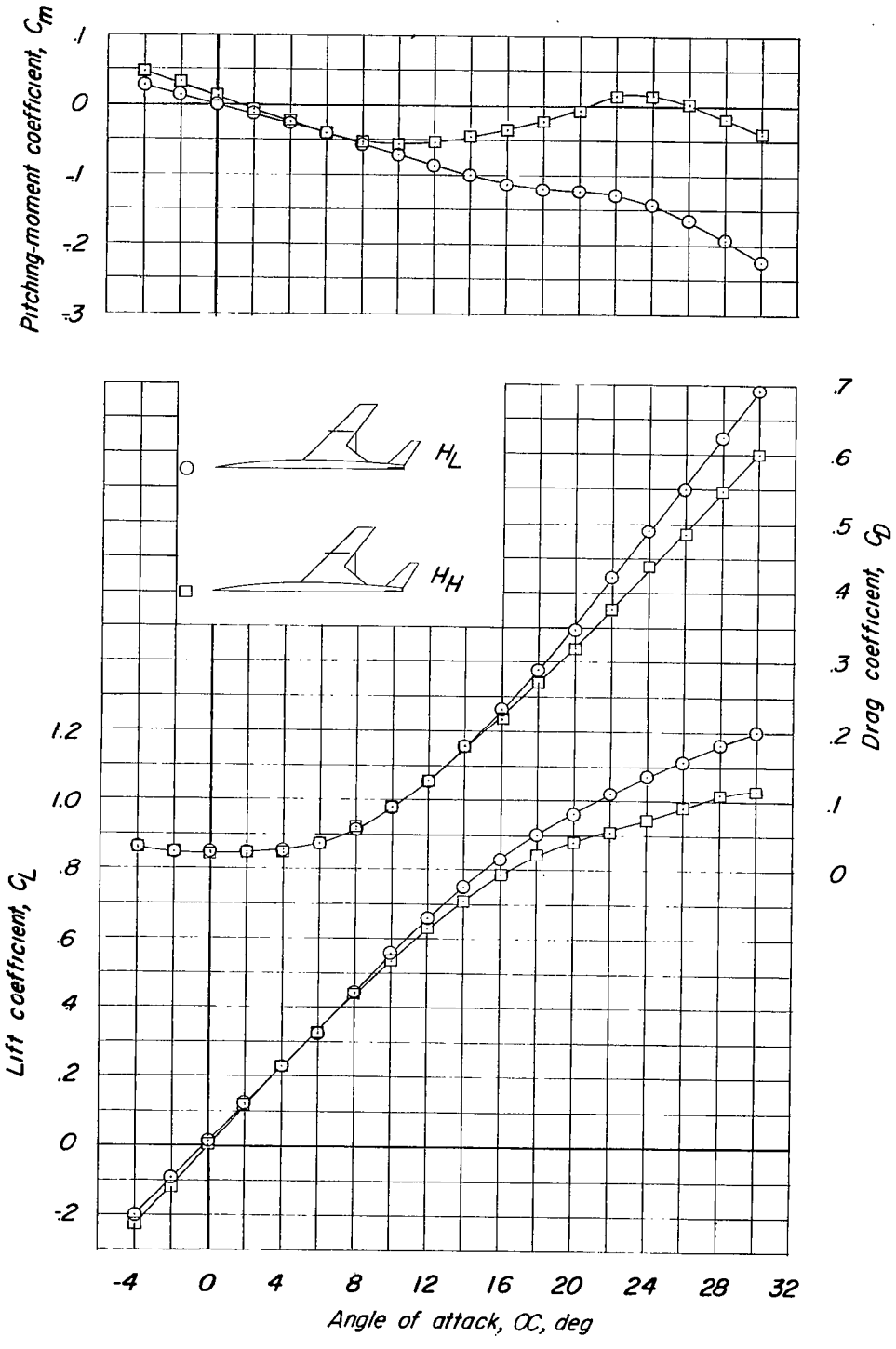

Figure 17.- Effect of horizontal-tail height on the static longitudinal stability characteristics of the complete model with fences f_2. M = 0.16.

[redacted]

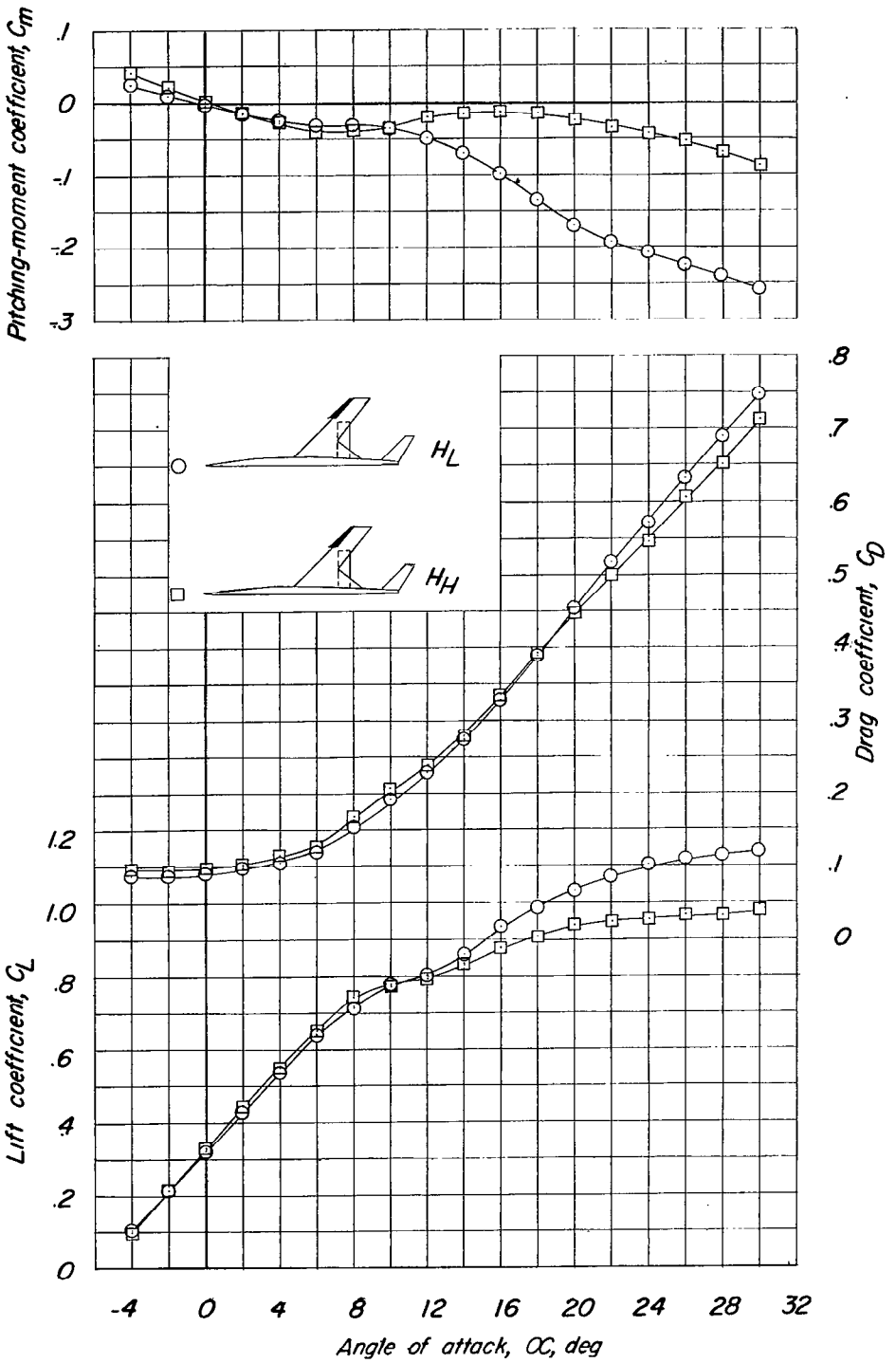

Figure 18.- Effect of horizontal-tail height on the static longitudinal stability characteristics of the complete model with flap B, $\delta = 40^\circ$, and slats s_1. M = 0.16.

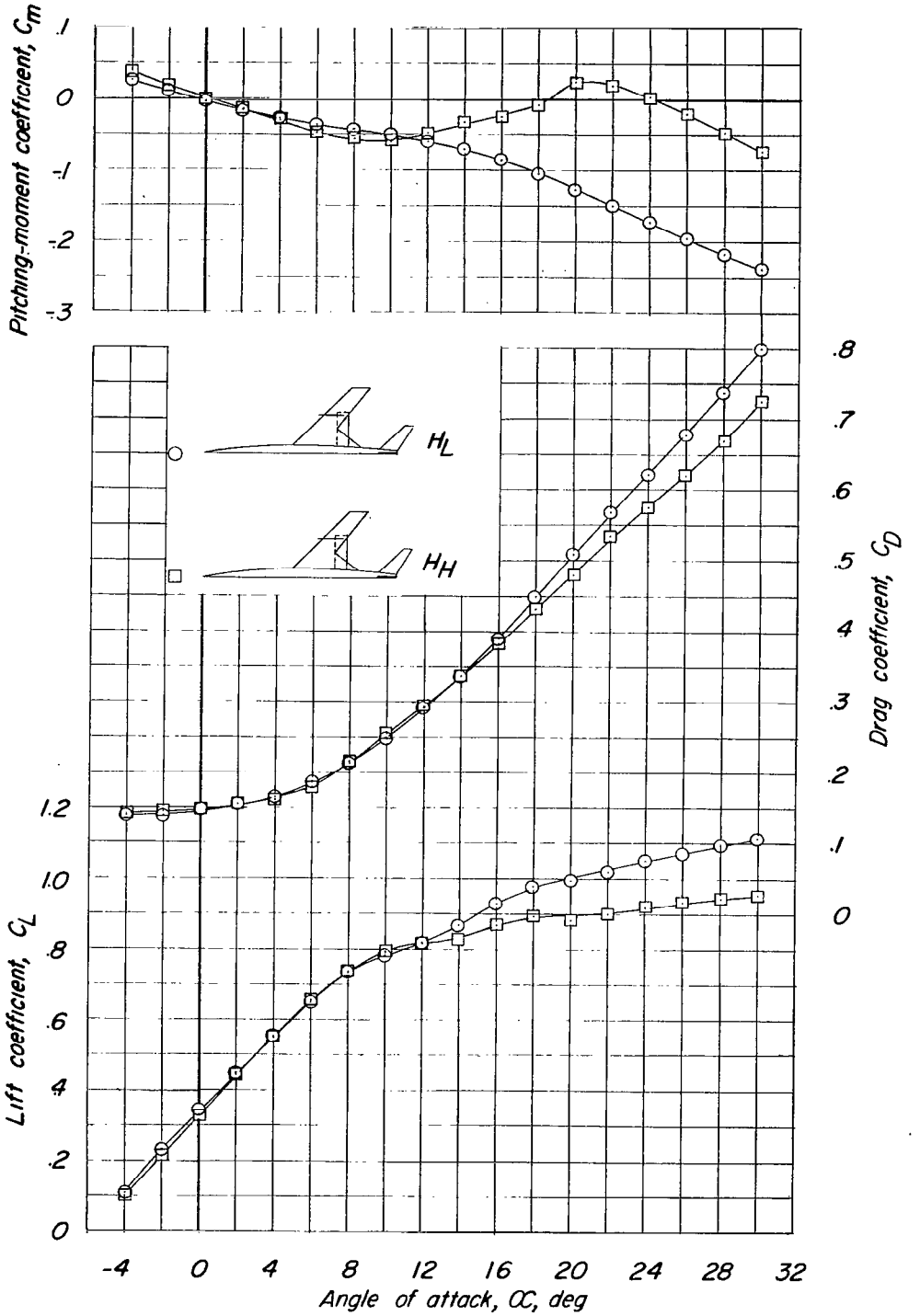

Figure 19.- Effect of horizontal-tail height on the static longitudinal stability characteristics of the complete model with flap B, $\delta = 40^\circ$, and fences f_2. M = 0.16.

[redacted]

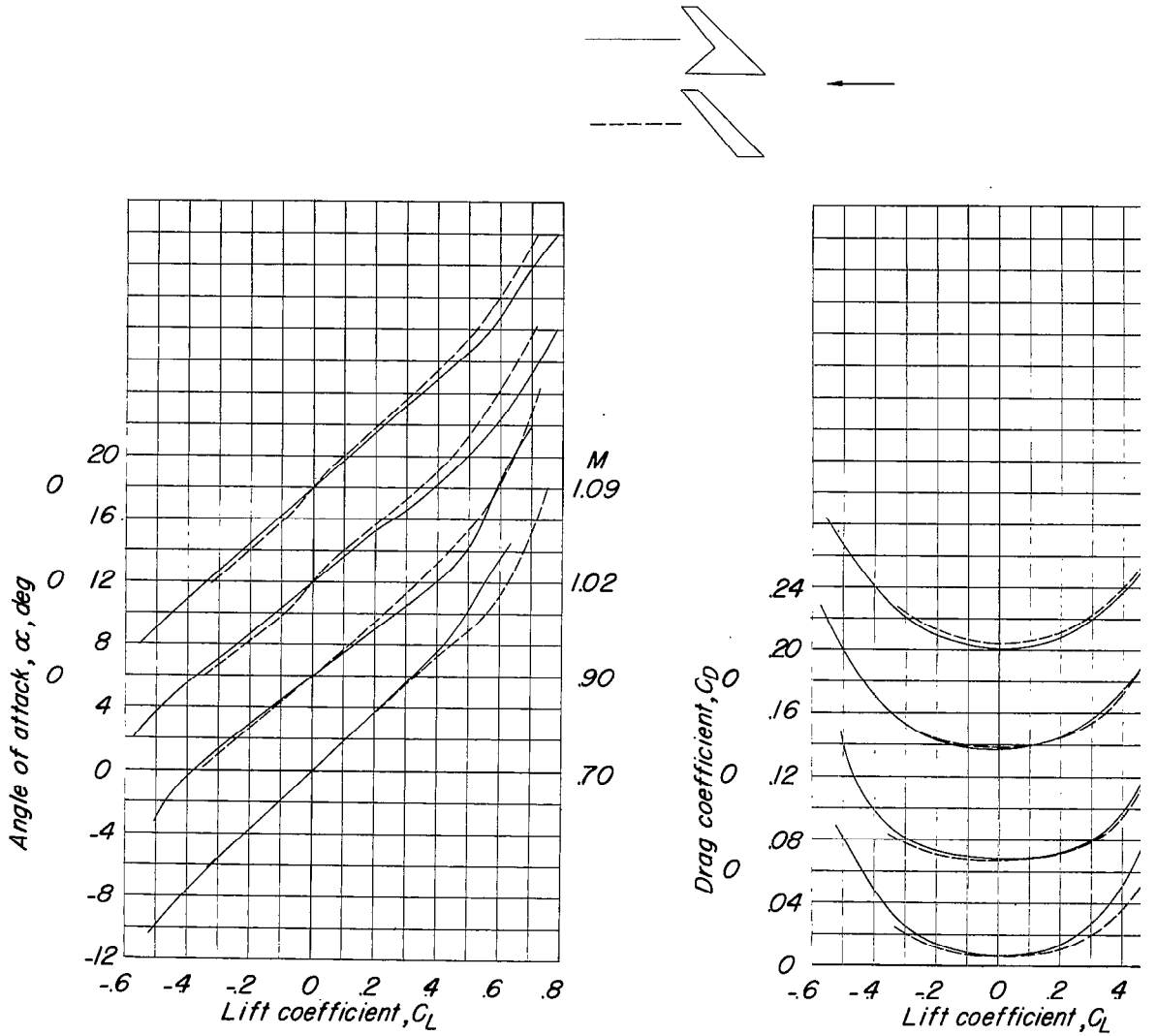

Figure 20.- Wing-alone high-speed static longitudinal stability chars teristics for conventional sweptback wing and composite-plan-form

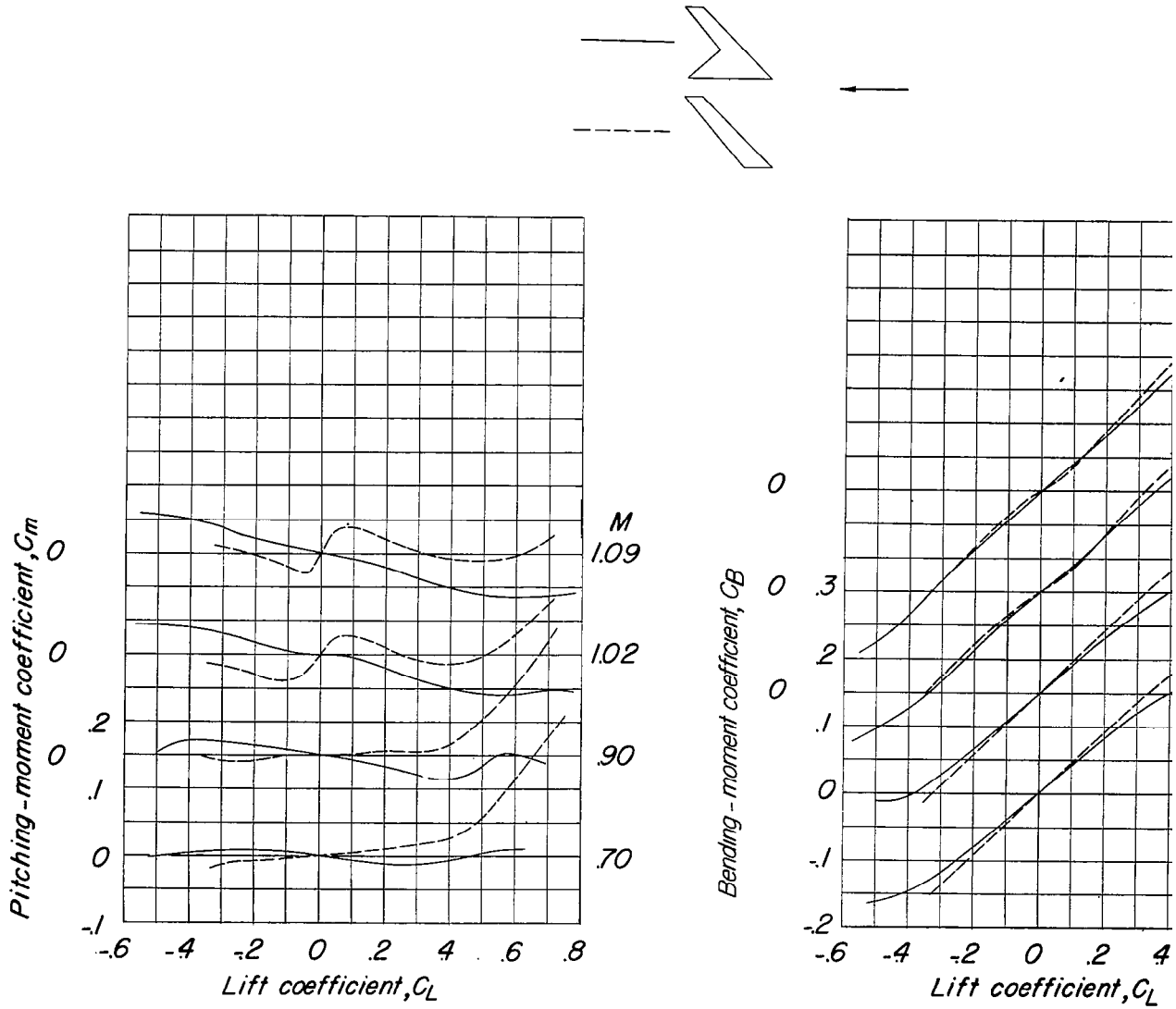

Figure 20.- Concluded.

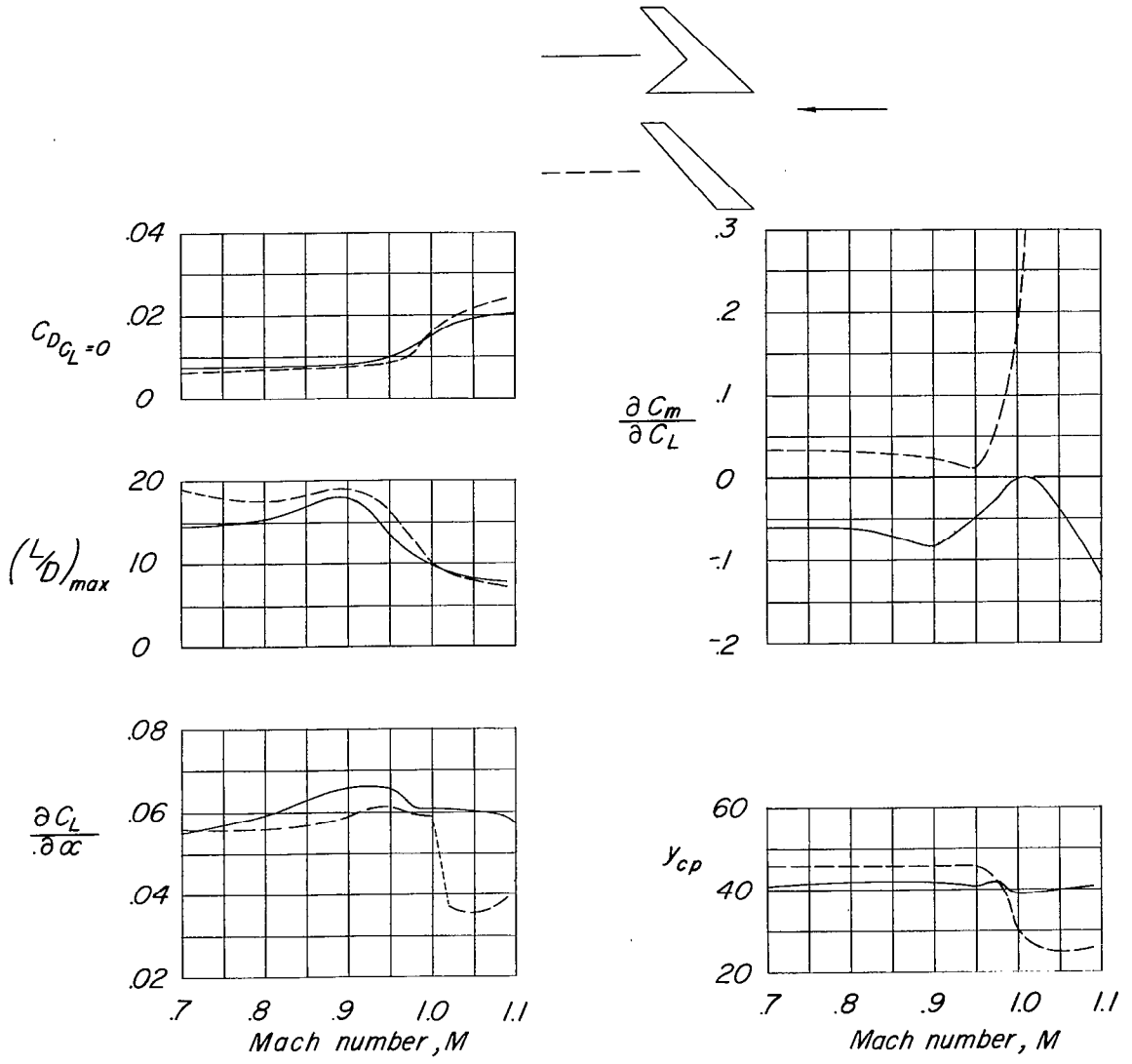

Figure 21.- Summary of wing-alone high-speed aerodynamic characteristics for conventional sweptback wing and composite-plan-form wing.

NACA-Langley - 8-18-54 - 350